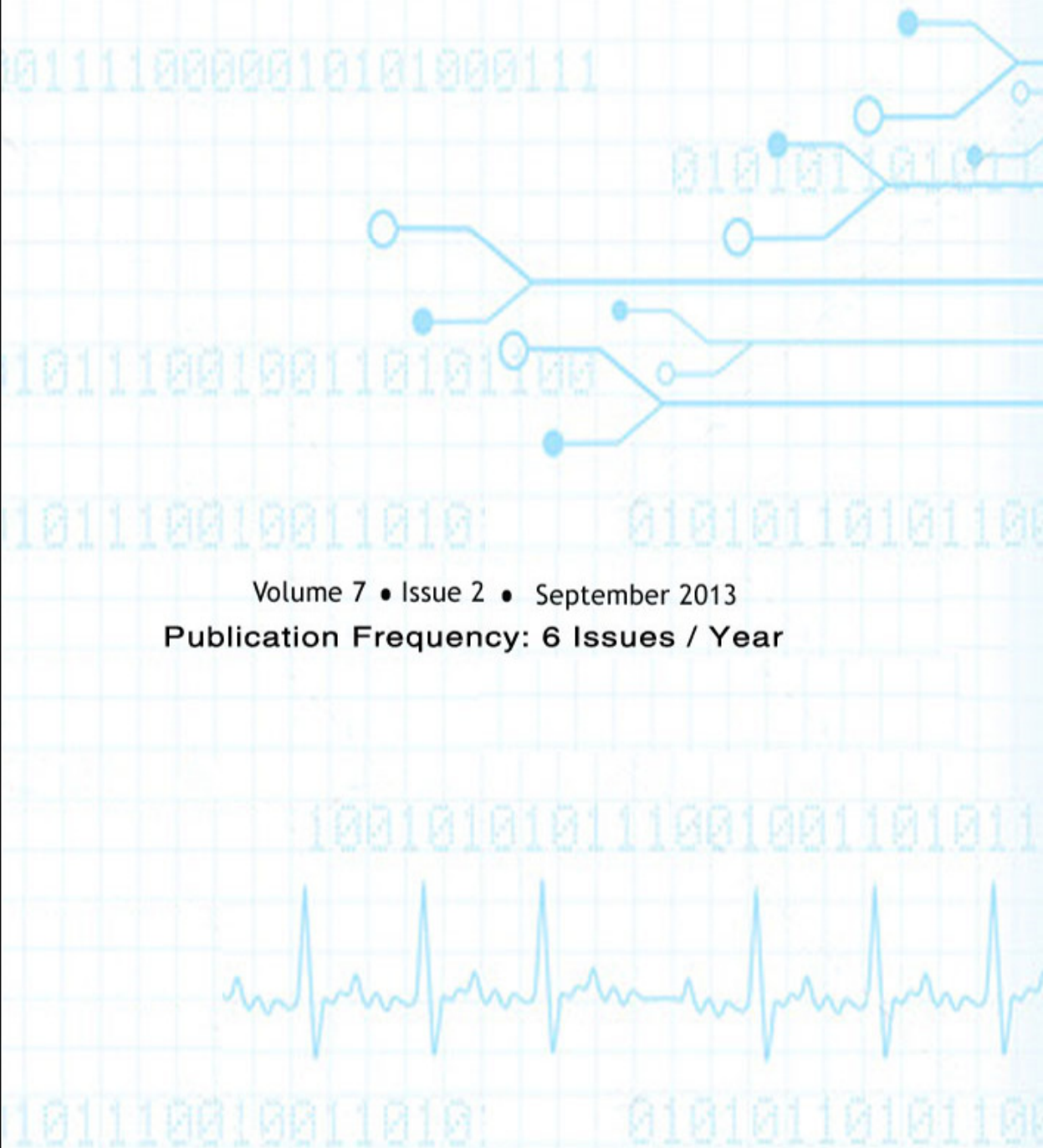


Editor-in-Chief
Dr Saif alZahir

SIGNAL PROCESSING (SPIJ)

AN INTERNATIONAL JOURNAL

ISSN : 1985-2339



Volume 7 • Issue 2 • September 2013

Publication Frequency: 6 Issues / Year

CSC PUBLISHERS
<http://www.cscjournals.org>

Copyrights © 2013 Computer Science Journals. All rights reserved.

SIGNAL PROCESSING: AN INTERNATIONAL JOURNAL (SPIJ)

VOLUME 7, ISSUE 2, 2013

**EDITED BY
DR. NABEEL TAHIR**

ISSN (Online): 1985-2339

International Journal of Computer Science and Security is published both in traditional paper form and in Internet. This journal is published at the website <http://www.cscjournals.org>, maintained by Computer Science Journals (CSC Journals), Malaysia.

SPIJ Journal is a part of CSC Publishers

Computer Science Journals

<http://www.cscjournals.org>

SIGNAL PROCESSING: AN INTERNATIONAL JOURNAL (SPIJ)

Book: Volume 7, Issue 2, September 2013

Publishing Date: 15 - 09 - 2013

ISSN (Online): 1985-2339

This work is subjected to copyright. All rights are reserved whether the whole or part of the material is concerned, specifically the rights of translation, reprinting, re-use of illustrations, recitation, broadcasting, reproduction on microfilms or in any other way, and storage in data banks. Duplication of this publication of parts thereof is permitted only under the provision of the copyright law 1965, in its current version, and permission of use must always be obtained from CSC Publishers.

SPIJ Journal is a part of CSC Publishers

<http://www.cscjournals.org>

© SPIJ Journal

Published in Malaysia

Typesetting: Camera-ready by author, data conversion by CSC Publishing Services – CSC Journals, Malaysia

CSC Publishers, 2013

EDITORIAL PREFACE

This is Second Issue of Volume Seven of the Signal Processing: An International Journal (SPIJ). SPIJ is an International refereed journal for publication of current research in signal processing technologies. SPIJ publishes research papers dealing primarily with the technological aspects of signal processing (analogue and digital) in new and emerging technologies. Publications of SPIJ are beneficial for researchers, academics, scholars, advanced students, practitioners, and those seeking an update on current experience, state of the art research theories and future prospects in relation to computer science in general but specific to computer security studies. Some important topics covers by SPIJ are Signal Filtering, Signal Processing Systems, Signal Processing Technology and Signal Theory etc.

The initial efforts helped to shape the editorial policy and to sharpen the focus of the journal. Started with volume 7, 2013, SPIJ appears with more focused issues related to signal processing studies. Besides normal publications, SPIJ intend to organized special issues on more focused topics. Each special issue will have a designated editor (editors) – either member of the editorial board or another recognized specialist in the respective field.

This journal publishes new dissertations and state of the art research to target its readership that not only includes researchers, industrialists and scientist but also advanced students and practitioners. The aim of SPIJ is to publish research which is not only technically proficient, but contains innovation or information for our international readers. In order to position SPIJ as one of the top International journal in signal processing, a group of highly valuable and senior International scholars are serving its Editorial Board who ensures that each issue must publish qualitative research articles from International research communities relevant to signal processing fields.

SPIJ editors understand that how much it is important for authors and researchers to have their work published with a minimum delay after submission of their papers. They also strongly believe that the direct communication between the editors and authors are important for the welfare, quality and wellbeing of the Journal and its readers. Therefore, all activities from paper submission to paper publication are controlled through electronic systems that include electronic submission, editorial panel and review system that ensures rapid decision with least delays in the publication processes.

To build its international reputation, we are disseminating the publication information through Google Books, Google Scholar, Directory of Open Access Journals (DOAJ), Open J Gate, ScientificCommons, Docstoc and many more. Our International Editors are working on establishing ISI listing and a good impact factor for SPIJ. We would like to remind you that the success of our journal depends directly on the number of quality articles submitted for review. Accordingly, we would like to request your participation by submitting quality manuscripts for review and encouraging your colleagues to submit quality manuscripts for review. One of the great benefits we can provide to our prospective authors is the mentoring nature of our review process. SPIJ provides authors with high quality, helpful reviews that are shaped to assist authors in improving their manuscripts.

Editorial Board Members

Signal Processing: An International Journal (SPIJ)

EDITORIAL BOARD

EDITOR-in-CHIEF (EiC)

Dr Saif alZahir

University of N. British Columbia (Canada)

ASSOCIATE EDITORS (AEiCs)

Professor. Wilmar Hernandez

Universidad Politecnica de Madrid
Spain

Dr Tao WANG

Universite Catholique de Louvain
Belgium

Dr Francis F. Li

The University of Salford
United Kingdom

EDITORIAL BOARD MEMBERS (EBMs)

Dr Jan Jurjens

University Dortmund
Germany

Dr Jyoti Singhai

Maulana Azad National institute of Technology
India

Assistant Professor Weimin Huang

Memorial University
Canada

Dr Lihong Zhang

Memorial University
Canada

Dr Bing-Zhao Li

Beijing Institute of Technology
China

Dr Deyun Wei

Harbin Institute of Technology
China

TABLE OF CONTENTS

Volume 7, Issue 2, September 2013

Pages

- 96 - 109 DrCell – A Software Tool for the Analysis of Cell Signals Recorded with Extracellular Microelectrodes
Christoph Nick, Michael Goldhammer, Robert Bestel, Frederik Steger, Andreas Daus, Christiane Thielemann
- 110 - 116 Construction of The Sampled Signal Up To Any Frequency While Keeping The Sampling Rate Fixed
Ziad A Sobih, Prof. Martin Schetzen
- 117 - 130 Rule Based Identification of Cardiac Arrhythmias from Enhanced ECG Signals Using Multi-Scale PCA
Sharmila Vallem, Ette Hari Krishna, Komalla Ashoka Reddy

DrCell – A Software Tool for the Analysis of Cell Signals Recorded with Extracellular Microelectrodes

Christoph Nick

*Department of Engineering, biomems lab
University of Applied Sciences Aschaffenburg,
63743 Aschaffenburg, Germany*

Christoph.nick@h-ab.de

Michael Goldhammer

*Department of Engineering, biomems lab
University of Applied Sciences Aschaffenburg,
63743 Aschaffenburg, Germany*

Michael.goldhammer@h-ab.de

Robert Bestel

*Department of Engineering, biomems lab
University of Applied Sciences Aschaffenburg,
63743 Aschaffenburg, Germany*

Robert.bestel@h-ab.de

Frederik Steger

*Department of Engineering, biomems lab
University of Applied Sciences Aschaffenburg,
63743 Aschaffenburg, Germany*

Frederik.steger@hotmail.de

Andreas W. Daus

*Department of Engineering, biomems lab
University of Applied Sciences Aschaffenburg,
63743 Aschaffenburg, Germany*

Andreas.daus@h-ab.de

Christiane Thielemann

*Department of Engineering, biomems lab
University of Applied Sciences Aschaffenburg,
63743 Aschaffenburg, Germany*

christiane.thielemann@hotmail.de

Abstract

Microelectrode arrays (MEAs) have been applied for in vivo and in vitro recording and stimulation of electrogenic cells, namely neurons and cardiac myocytes, for almost four decades. Extracellular recordings using the MEA technique inflict minimum adverse effects on cells and enable long term applications such as implants in brain or heart tissue.

Hence, MEAs pose a powerful tool for studying the processes of learning and memory, investigating the pharmacological impacts of drugs and the fundamentals of the basic electrical interface between novel electrode materials and biological tissue. Yet in order to study the areas mentioned above, powerful signal processing and data analysis tools are necessary.

In this paper a novel toolbox for the offline analysis of cell signals is presented that allows a variety of parameters to be detected and analyzed. We developed an intuitive graphical user interface (GUI) that enables users to perform high quality data analysis. The presented MATLAB® based toolbox gives the opportunity to examine a multitude of parameters, such as spike and neural burst timestamps, network bursts, as well as heart beat frequency and signal propagation for cardiomyocytes, signal-to-noise ratio and many more. Additionally a spike-sorting tool is included, offering a powerful tool for cases of multiple cell recordings on a single microelectrode.

For stimulation purposes, artifacts caused by the stimulation signal can be removed from the recording, allowing the detection of field potentials as early as 5 ms after the stimulation.

Keywords: MATLAB® Toolbox, Bio Signal Processing, Spike Sorting, Network Analysis, Extracellular Recording.

1. INTRODUCTION

For all neural or cardiac implants, cell activity is detected by extracellular electrodes in the form of field potentials. Since cortical implants might be used someday to control artificial limbs, wheelchairs or software [1, 2], improving the living conditions of disabled people, the field of neural signal processing is of utmost importance.

Yet signal processing is not only essential for in vivo applications such as implants, but also for in vitro studies of neural as well as cardiac networks that require substantial amounts of data processing. These systems are a powerful tool for studying learning, memory [3] and pharmacologic mechanisms [4]. In addition, the properties of the interface between novel electrode materials and biological tissue can be investigated [5], especially as there has been a growing community utilizing different kinds of multi-electrode arrays for in vivo and in vitro experiments in the recent past. Although the MEAs being used may differ in electrode size, substrate and electrode material as well as in number of electrodes, they all share the same working principles: (1) extracellular microelectrodes do not penetrate the cell membrane. (2) They record field potentials in the vicinity of the cell caused by changes in membrane potential – so called action potentials (AP). (3) The cells are either cultured onto the electrode array for in vitro studies or the chip is implanted into living tissue for in vivo studies. (4) These electrodes can be used to stimulate cells through voltage or current pulses.

There are a couple of software toolboxes for neuronal signal processing available, where only a few are specifically designed for extracellular signals recorded by microelectrode arrays. These toolboxes include the commercially available MC_Rack (multichannel systems, Reutlingen, Germany), NeuroExplorer (Nex Technologies, Littleton, MA, USA), Offline Sorter (Plexon, Dallas, TX, USA) or NeuroMAX (R.C. Electronics Inc, Santa Barbara, CA, USA) and, furthermore, the open source projects FIND [6] sigTool [7] or nStat [8] to name only a few. Most of these toolboxes focus on neural signal processing exclusively, whereas cardio tools have not received as much attention. This motivated us to develop an open toolbox including established as well as new algorithms like a novel spike sorting algorithm that enable analysis of a variety of parameters for neural and cardiac cell signals.

In the following we introduce an offline signal processing toolbox with algorithms for spike and burst detection, a sophisticated algorithm for spike sorting, spike overlay and signal propagation for cardiac cells and furthermore an analysis of simultaneous neural network activity.

There are several cells that can change their resting potential e.g. neurons and cardiac myocytes. Throughout this paper we use the term spike to describe such a voltage peak no matter which cell caused it. Since the software tool reported herein is capable of working with any kind of spike we do not distinguish between different kinds of cell signals.

This multi domain approach combined with powerful tools for neural and cardiac signals is unique in the field of offline analysis of electrophysiological data.

The GUI, provides researchers an easy to use platform to process their signals and test new, custom made algorithms. A flow chart of available processing steps is shown in Figure 1. Generally the algorithms are designed for microelectrode arrays with 60 electrodes, yet signals originating from other set ups such as needle arrays or arrays with a different number of working electrodes can be processed as well.

The software is distributed under the GNU general public license (GPL) version 3 and is available from the authors at www.h-ab.de/drcell. It is based on MATLAB® R2012a including the Curve Fitting, Image Processing, Signal Processing, Statistics and Wavelet toolboxes.

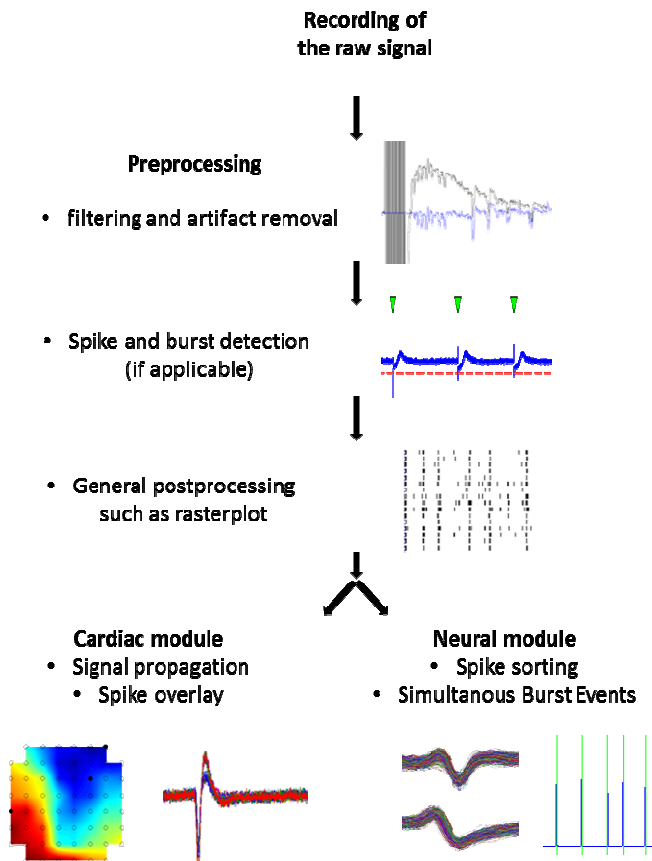


FIGURE 1: Flow chart of possible processing steps in the “DrCell” software toolbox.

To test the developed algorithms cell culture experiments were conducted. Data recording was done using a multichannel system amplifier stage combined with custom made LabVIEW™ based software. Details about cardiac cell cultures can be found in [5] Details about neural cell cultures in [9]. In short, cortical rat neurons were purchased cry conserved from Lonza Ltd (Lonza Ltd, Basel, Switzerland). Before cultivation, microelectrode arrays were coated with Poly-D-Lysine (PDL, 0,1 mg/ml in phosphate buffered saline (PBS), Sigma-Aldrich Chemie GmbH, Taufkirchen, Germany) and Laminin (15 µg/ml in PBS, Sigma-Aldrich Chemie GmbH). Spikes were recorded from day 14 in vitro.

Cardiac myocytes were prepared from chick embryos (E8). Hearts were carefully removed, the tissue dissociated and the cells cultured onto the MEAs. Here the chips were coated with Fibronectin (10 µg/ml in PBS, Sigma-Aldrich Chemie GmbH) prior to cultivation.

2. RESULTS AND DISCUSSION

The software tool named “DrCell” is subdivided into general preprocessing tools and a specific module for cardiomyocytes as well as a module designed for neural signal processing and analysis. While the cardiac module includes algorithms to analyze the contraction rate of the

tissue and signal propagation across the electrode array, the neural module features algorithms developed to analyze bursts and network behavior.

2.1 Preprocessing

In order to enable or just improve the detectability of signal parameters, it is advantageous to apply preprocessing algorithms to the recorded data. This includes digital filtering, spike detection and spike sorting for neuronal signals as well as the removal of stimulation artifacts in the case of an electrical stimulation.

The graphical user interface of the MATLAB® software tool allows loading of ASCII files, containing recorded data, into the workspace for further processing. If the data is not recorded in ASCII file format it must first be converted using freely available tools such as the MC_DataTool from multichannel systems.

In a first step the signal can be filtered by a bandstop or a bandpass filter. The frequencies for the lower and upper stopband edge frequencies can be set manually by the user. If both values are identical a notch filter with 1 dB passband ripple is applied at the chosen frequency. For the bandfilter an IIR Chebyshev filter with 20 dB stop band attenuation and ripple in the stopband is used.

In addition, noisy electrodes can be omitted completely and stimulation artifacts can be removed as described in detail later. The next processing steps include the calculation of thresholds, spike and burst detection as well as several post processing tools such as spike sorting, analysis of network bursts, correlation analysis and spike shape analysis.

2.2 Spike Detection

The overall quality of the data analysis depends on the reliability of spike detection. Only if spikes are detected correctly, bursts, simultaneous bursts (bursts that appear over multiple electrodes at the same time), interspike intervals, or shapes of spikes can be detected and analyzed correctly. Out of a broad variety of spike detection methods, the first reported and still widely applied algorithm uses a negative multiple of the root mean square (rms), or alternately of the standard deviation of the base noise, as threshold. If the signal voltage drops below this value, a spike is detected [10]. Variations of this very easy, fast and reliable algorithm are also available e.g. multiple thresholds [11] or in combination with additional pattern recognition algorithms [12].

The spike detection algorithm implemented in DrCell works in four steps, which are summarized here and explained in detail below: (1) A time frame of two seconds on each electrode containing exclusively noise is detected. (2) For this frame the root mean square (rms) value and the standard deviation are calculated and (3) multiplied with a negative factor. As default value a multiple of the rms is used as threshold; alternatively a multiple of the standard deviation can be chosen instead. (4) The absolute minimum of every voltage peak that is lower than the threshold is saved as the spike's timestamp.

(1) To detect the base noise level, a time window is shifted over the signal of each channel searching for spike-free periods. The size of the window is set to 50 ms as default value but can be adjusted by the user. The detection of spike free windows is achieved by fitting the signal histogram with a Gaussian distribution, typical for white noise. A low standard deviation (equal or lower than a value defined by the user and set as default to ≤ 5) from this Gaussian distribution is interpreted as pure, spike-free noise. In this case the noise data is saved in a separate array and the window is shifted forward by one window length. If the standard deviation is higher than the defined value spikes are likely to be present in that particular interval and the window is only shifted half the window length and conditions are checked again. This process is repeated until a time period of 2 seconds is identified as "spike-free". Sometimes the signal-to-noise ratio is too low for any signal to be detected. If half of the total recording time has been swept and no spike-free window has been found, the algorithm stops and this particular electrode is labeled "noisy", hence being disregarded for any further analysis.

As an option, the user can also define the timeframe to be used for calculating the rms value or standard deviation of the noise manually.

(2-3) The rms value or, respectively, the standard deviation of these spike free signal arrays is multiplied by an empiric factor of -6 (default value) to set the threshold. This factor can also be set manually in the range of -3 to -14.

In addition, a refractory time between spikes can be defined, if wished by the user. In this case the algorithm works as defined above but, after saving all timestamps, the intervals between the spikes are checked for physiological plausibility and, if this is not given, the second spike is erased from the array.

The signal-to-noise ratio (SNR) of biological signals is not easily determined. In general the SNR is defined as the signal-power divided by the noise-power. Since only field potentials are measured, in other words voltage signals, there is no information on the respective power. Therefore we define the SNR of each electrode as $SNR = (v_{ps}/\sigma_n)^2$, while v_{ps} describes the average peak voltage of spikes and σ_n the standard deviation of the noise [5]. By assuming the same impedance for signal and noise amplitudes the power ratio is calculated by squaring the fractal expression.

This algorithm provides a very reliable and fast method for spike detection and is also easily implementable for online analysis.

2.3 Stimulation Artifact Removal

If cells are stimulated by electrical impulses supplied by a current or a voltage source [3], cell responses may be superimposed by undesirable distortions. Here we distinguish between crosstalk originating from the stimulation signal itself (about -18 ms to 0 ms in Fig. 3) and artifacts that appear shortly after the stimulation (about 0 ms until 80 ms in Fig. 3). Typically, cell reactions to the stimulation are expected within the first few milliseconds after the end of stimulation, while artifacts last up to 100 ms; therefore the removal of artifacts is desirable [13]. There are several approaches to achieve cancellation of artifacts described in the literature: the separation of stimulation and recording electrodes [14], the application of sample and hold elements [15], pass filters [16] or algorithms to restore the disturbed signal [13, 17].

The algorithm implemented in the DrCell toolbox reduces the critical time after a stimulus from about 100 ms to below 10 ms. For this purpose the beginning and end of the stimulation period is detected by a threshold based algorithm. The artifact signal is fitted by two consecutive 9th order polynomials, one for the period between 0.5 and 7.5 ms and one for 7.5 to 82.5 ms after stimulation. Subtraction of these polynomials from the recorded signal reduces distortions significantly (see Figure 2). In case the first couple of milliseconds (1 - 5 ms) are severely distorted, this time interval may be completely removed (set to 0 V), just as the stimulation interference itself.

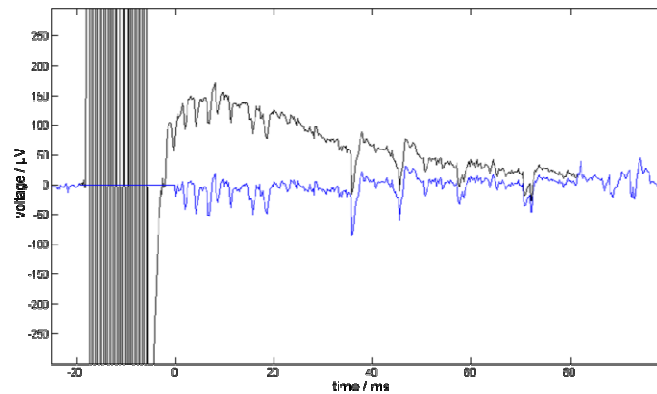


FIGURE 2: Effect of artifact removal. Stimulation crosstalk (-18 ms to 0 ms) and artifacts (about 0 ms until 80 ms) are removed from the distorted original signal (black) resulting in an adjusted signal (blue). This step clearly facilitates the spike detection immediately after stimulation.

According to Ruaro [16] applying ninth order polynomials will result in robust artifact removal, while higher order polynomials would unnecessarily increase the computation cost. The application of polynomials of lesser order can still result in corrupted artifact removal.

Cardiac Module

2.4 Beat Rate

Regular and synchronous contraction is a key feature of cardiac tissue. Pacemaker cells have the ability to initiate action potentials that propagate via gap junctions within a functional syncytium. In cardiac myocytes cultured on MEAs, the contraction rate correlates over time with the intrinsic field potentials and thus can be analyzed in terms of beat rate or for possible arrhythmias [18]. In our experiments, the former is calculated by the reciprocal median of the Interspike intervals (ISIs). The regularity is estimated using the median absolute deviation (MAD) of reciprocal ISIs [19].

2.5 Spike Shape and Propagation

Typically the course of field potentials can be divided into several phases identified by negative or positive peaks, respectively. Applying chemical or electrical stimuli to the cells, as well as the effects of aging may influence several characteristics of the spike shape, e.g. the general field action potential duration, amplitude or the repolarization time. Therefore some domains might be prolonged or reduced and might occur either delayed or prematurely, respectively, whereas some characteristics of spike shape may become less distinctive or may even disappear.

In cultures of cardiac tissue, the signal generated by pacemaker cells spreads throughout the whole network. As a consequence it is interesting to investigate the origin, direction and propagation speed of the specific signal. For this purpose an algorithm is implemented that maps almost synchronous spikes in a false color map by applying a time scale in the two dimensions of the electrode array (Figure 3 top). Noisy electrodes without discernible spikes or electrodes manually omitted from the analysis are highlighted in black. To further facilitate propagation pathway identification, arrows may be superimposed indicating propagation direction and speed (length of the arrows), not shown.

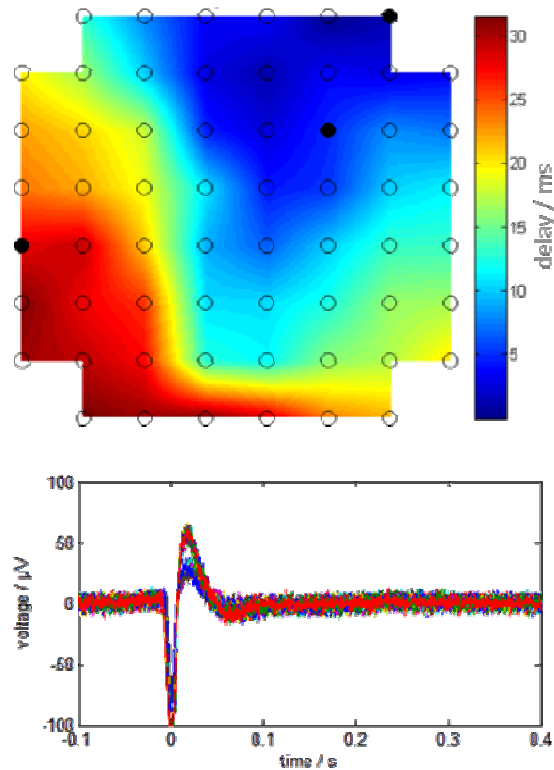


FIGURE 3: Propagation and spike overlay. The propagation of one heartbeat over the electrode array is shown (top). A spike overlay is displayed, where two different spike forms can clearly be distinguished (bottom).

The propagation algorithm is based on the detection of the first spike appearing on the MEA. Delayed spikes within the next 200 ms are identified and their retard and electrode position are used to calculate speed and propagation pathways which are visualized on a virtual MEA layout.

To address the issue of varying spike shapes, the DrCell algorithm determines characteristic peaks of each spike and the interval between these peaks. In addition, these data are not only calculated for just one spike, but may either be assessed for all spikes recorded by a single electrode or as mean values of the spikes recorded by all electrodes, further including information about their standard deviation and median. A graphic panel depicts an overlay of all spikes recorded on a single electrode (Figure 3 bottom), allowing an easy assessment of continued conformity of the spike shapes. The algorithm uses detected spikes and displays a time frame [spike time - x; spike time + y] of each selected spike.

This panel proves especially valuable when working with cardiac tissues, as comparison of the duration of the field action potentials presents a valid method to evaluate the risk of diverse heart diseases. Of course, observation of single spikes is an option as well. In this case, the user may switch from one recorded spike to the next receiving single spike data, also allowing manual query of time points during the measurement.

With these tools at hand the electrophysiological effects of aging, electrical or pharmacologic stimuli can be easily detected and tracked throughout the course of experiment.

Neural Module

2.6 Spike Sorting

With a typical electrode diameter of 20 - 30 μm , each electrode is capable of recording signals from several cells at once. Especially for neural cell cultures it is crucial to identify the network activity on a single cell level, as subsequent analysis, such as burst or network burst detection, is

primarily based on this information. Under the assumption that the coupling between an individual cell and its respective electrode creates a unique spike shape characteristic, several pattern-matching methods, called spike-sorting algorithms, have been developed in order to address this task. The DrCell framework provides a unique spike-sorting algorithm for this purpose, which is described in detail in [20].

Unlike other spike sorting algorithms that exclusively use a specific type of feature, such as principal components [21, 22] or certain Wavelet based coefficients [23], the implemented algorithm calculates a variety of features and chooses the most suitable in a subsequent step. In order to distinguish the features most suitable for discriminating the spike shapes present in the recorded signal, the probability distribution of each derived feature is calculated over all detected spikes. The distributions are then evaluated with the expectation maximization algorithm (EM) that approximates the derived probability functions with a mixture of Gaussians. This allows an identification of multimodal distributed features that have the potential of discriminating different spike shapes. The features with the most distinguishable multimodal character are chosen for the final clustering step, with the correlation between the particular features serving as an additional criterion. In the last step the spikes are clustered into distinct groups on the basis of the determined set of features. Many sorting algorithms differ not only in the chosen set of features but also in their classification methods, and either use simple clustering, e.g. k-means [20], fuzzy c-means [22] or superparamagnetic clustering [23] or favor more complex classification algorithms using artificial neural networks [24] or support vector machines [25]. Since the latter classification algorithms usually require extensive and difficult training with specifically designed data, an expectation maximization clustering method was chosen in this context, as this approach fits best into the overall spike sorting algorithm. As shown in Figure 4, the described spike sorting process allows the discrimination of different spike shapes, in other words different cell signals, from each other.

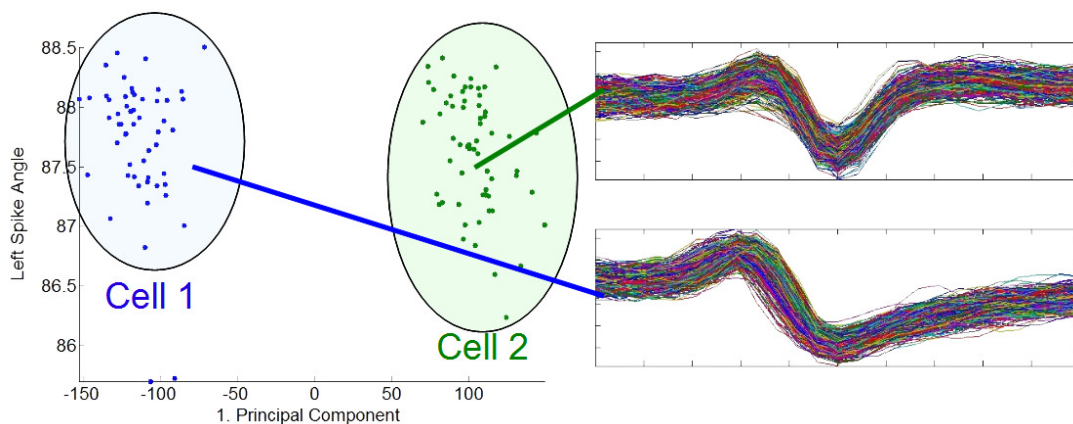


FIGURE 4: Sorting result for two spiking neurons recorded by one electrode. Two different spike shapes can clearly be distinguished.

Thus, the results of any following analysis of network activity or network information processing can be significantly enhanced and more detailed interpretation is possible.

2.7 Burst Detection

The definition of a burst varies in the literature, but most sources use already detected spikes to find possible burst events. Since there is no commonly accepted definition, we describe some definitions from the literature and then explain the implemented algorithms in detail. It should be mentioned that each definition has consequences with regard to the number and time of detected bursts and thus may alter the results.

One of the oldest methods to detect a burst is based on purely statistical means. A burst is found in this case by analyzing the interspike intervals (ISIs). An unexpected series of short ISIs is then defined as a burst [26].

In contrast to this approach, there are several definitions stating that a burst consists of a certain number of spikes within a specific timeframe. Turnbull defines a burst as a series of 2–5 spikes with a maximum interspike interval of 12-50 ms, with the exact value of these parameters being adjustable according to individual needs [27]. Chagnac-Amital defines a burst as a series of at least three spikes, with no interspike interval being set [28]. Martinoia and Chiappalone both define a burst as a series of at least 10 spikes, with the interval between two spikes not exceeding 100 ms [10, 29]. Corner defines several kinds of bursts. A mini-burst is a series of at least three spikes with a maximum interspike interval of 100 ms, with only the spikes of a specific electrode being considered. A midi-burst is a series of at least three spikes with a maximum interspike interval of 1000 ms on more than one electrode [30]. Baker adds another burst-species – a micro burst. This kind of burst is a series of at least three spikes with a maximum interspike interval of 10 ms [31].

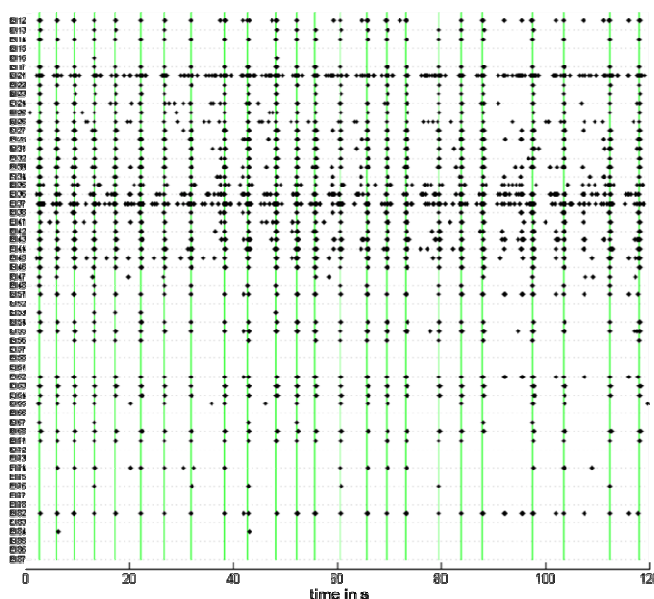


FIGURE 5: Raster plot of all recorded electrodes. Each spike is represented by one dot. Simultaneous burst events are marked by a green line.

According to Wagenaar, a burst is a group of spikes with a certain interspike interval [32]. The limit for the interspike interval is either 100 ms or $(4 \text{ times the average spike rate (spikes/second)} - 1)$, whichever is less. After four spikes with these parameters are found, the interspike interval is set to the minimum of $(3 \text{ times the average spike rate} - 1)$ and 200 ms and more spikes that meet these criteria are searched before and after this core group.

Jungblut defines a burst based on definitions by [10, 32] as a series of at least 3 spikes with the interspike interval of the first two spikes not exceeding 10 ms and with the ISI of the following spikes no longer than 20 ms [34].

Several of the algorithms mentioned above are implemented in the DrCell software. As default parameters we set a definition that is equivalent to Jungblut’s burst. The settings can be manually changed so that other definitions of bursts can also be used, e.g. the algorithm for Corner’s mini-burst or the definition of Wagenaar with at least 3 or 4 spikes per burst. For analyzing cardiac cells there is no burst and the ISI interval can be set to either 100 ms or 200 ms. All definitions are only default values and can be adjusted as the operator wishes.

The first spike of the burst is taken as the burst timestamp and the time difference between the first and last spike is saved as the burst duration. The interburst interval is calculated between the last spike of the n th burst and the first spike of the $(n+1)$ th burst. These values are calculated and saved as averages with standard deviation for each channel and for all channels. Furthermore, the average number of spikes per burst is saved for each electrode as well as for the whole electrode array. The detected spikes and bursts are marked in the signal and can be viewed additionally as a spike train or as a raster plot (Figure 5).

2.8 Network Behavior

The occurrence of simultaneous burst events (SBEs) as shown in Figure 6 can be seen as an indicator of the connections and communication within the neural network.

A burst is typically generated in a certain area of the network and then spreads across the whole array, which leads to nearly simultaneous bursts at multiple electrodes. Depending on how well a neural network is connected, these synchronous events occur rarely to frequently (1 – 30 per minute) and show different speeds of propagation [35].

Because of the large number of possible connections (each cell on the chip can form up to 10,000 synapses) between the neurons and thus the possible paths the signal can propagate, it is impossible to determine the exact pathway by evaluating the burst timestamps on the various electrodes.

However, by evaluating the direction of signal propagation, it can be determined whether network bursts consistently start from the same region and if they are propagated along similar pathways [36]. Further, the number of electrodes that are involved in a network burst and the time between the first and the last burst (propagation speed) can be evaluated.

Similar to regular bursts, there are different definitions of network bursts. Van Pelt assumes that the number of active electrodes and the spike rate of each electrode are increased if a network burst occurs. Thus, the product of the number of active electrodes and the total spike rate can serve as a detection criterion [37]. Other definitions use the already detected spikes and bursts instead, yet differ in the required number of electrodes that take part in the network event.

In the algorithm by Segev, at least 80% of all active electrodes must show activity within a 100 ms time window [38]. This algorithm proves to be reliable in general although we found that the criterion of at least 80% of all active electrodes being active simultaneously is very strict. Thus in DrCell the number of simultaneous active electrodes is set to five. After a burst has been detected, the algorithm checks for other active electrodes exhibiting a burst-event between 40 ms before and after the initially detected burst. If at least five such electrodes are found, the maximum of the resulting histogram of timestamps is called the network burst.

The histogram is then smoothened by a filter and the timestamps at 20% and 80% of the maximum before and after each network burst are saved. Based on these timestamps the rising time (20% - 80% before peak), the falling time (80% - 20% after peak) and the duration (20% before - 20% after) are calculated and saved. For the entire array all values are given with their minimum, maximum and average value including the standard deviation. Furthermore, the number of the participating electrodes is also stored, making a comparison between experiments straightforward.

Finally, in order to evaluate the similarity between two electrodes, the cross correlation can be calculated. The correlation is quantified by Cohen's Kappa, with a general value range between 0, meaning no correlation at all, and 1 meaning complete equality [39]. Additionally, the auto correlation can be calculated to evaluate the regularity of spikes or bursts.

3. CONCLUSION AND OUTLOOK

In this paper we present a software toolbox for the analysis of cell signals, regarding both neurons and cardiac cells that are recorded with microelectrode arrays. This toolbox thereby covers not only all basic processing algorithms such as spike detection, but also features a multitude of advanced algorithms for both neural and cardiac signals. It allows, for instance, the investigation of spike propagation behavior and, furthermore, the identification of single or multiple pacemaker centers in cardiomyocyte cultures. When faced with neuronal data, the toolbox provides a wide range of spike and burst analysis methods, such as spike sorting, burst and network burst analysis and even facilitates the handling of datasets recorded in stimulation experiments. Unlike many commercially available tools, the presented framework furthermore enables the user to customize or even add specific methods or features. This allows the user to alter, for example, the display of results according to individual needs or desires. It further permits the user to implement, for instance, new spike or burst criteria or even completely new processing methods in addition to the existing algorithms. New algorithms or functions can be called by prepared empty menu-buttons. Here Matlab, which is available at most research institutions, provides a very powerful environment to develop novel algorithms.

In the near future we will implement parts of this toolbox into our recording system for online analysis of cultured networks. Especially an online spikesorting algorithm will be very helpful for online analysis. We also plan to add more algorithms that will support the user in automatically analyzing sets of data and comparing their results. Further advancement of the algorithms include the propagation of signals over the array or analyzing network behavior by simulating neural networks with known mathematical models.

Furthermore the toolbox will serve as analytical tool for future cell culture tests, where the effects of radiation on the biological tissue are studied. In addition, recently developed Matlab® toolboxes such as the parallel computing toolbox allow various adaptations to Dr. Cell. As the presented software can be changed freely, this toolbox can be used to transform the Dr. Cell software into a GPU environment, processing individual electrodes independently and in parallel, hence speeding up the data analysis significantly.

ACKNOWLEDGMENTS

We want to thank M.E. Ruaro for his support with the implementation of the stimulation artifact algorithm. We would also like to thank Johannes Frieß for proofreading the manuscript. Furthermore, one of the authors (CN) would like to thank the Studienstiftung des deutschen Volkes for supporting his research.

4. REFERENCES

- [1] M. Nicoletis and J. Chapin, "Controlling robots with the mind," *Scientific American-American Edition*, vol. 287, no. 4, pp. 46–55, 2002.
- [2] M. Velliste, S. Perel, M. Spalding, A. Whitford, and A. Schwartz, "Cortical control of a prosthetic arm for self-feeding," *Nature*, vol. 453, no. 7198, pp. 1098–1101, 2008.
- [3] D. Wagenaar, R. Madhavan, J. Pine, and S. Potter, "Controlling bursting in cortical cultures with closed-loop multi-electrode stimulation," *Journal of Neuroscience*, vol. 25, no. 3, pp. 680–688, 2005.
- [4] A. Daus, P. Layer, and C. Thielemann, "A spheroid-based biosensor for the label-free detection of drug-induced field potential alterations," *Sensors and Actuators B: Chemical*, vol. 165, no. 1, pp. 53–58, 2012.

- [5] C. Nick, R. Joshi, J. Schneider, and C. Thielemann, "Three-dimensional carbon nanotube electrodes for extracellular recording of cardiac myocytes." *Biointerphases*, vol. 7, no. 1-4, pp. 58–64, 2012.
- [6] R. Meier, U. Egert, A. Aertsen, and M. Nawrot, "Find - a unified framework for neural data analysis," *Neural Networks*, vol. 21, no. 8, pp. 1085–1093, 2008.
- [7] M. Lidieth et al., "sigtool: A matlab-based environment for sharing laboratory-developed software to analyze biological signals," *Journal of neuroscience methods*, vol. 178, no. 1, pp. 188–196, 2009.
- [8] I. Cajigas, W. Malik, and E. Brown, "nstat: Open-source neural spike train analysis toolbox for matlab," *Journal of Neuroscience Methods*, vol. 211, no. 2, pp. 245—264, 2012.
- [9] C. Nick, S. Quednau, R. Sarwar, H.F. Schlaak and C. Thielemann, "High Aspect Ratio Gold Nanopillars on Microelectrodes for Neural Interfaces", submitted.
- [10] M. Chiappalone, A. Novellino, I. Vajda, A. Vato, S. Martinoia, and J. Van Pelt, "Burst detection algorithms for the analysis of spatio-temporal patterns in cortical networks of neurons," *Neurocomputing*, vol. 65, pp. 653–662, 2005.
- [11] T. Borghi, R. Gusmeroli, A. Spinelli, and G. Baranauskas, "A simple method for efficient spike detection in multiunit recordings," *Journal of neuroscience methods*, vol. 163, no. 1, pp. 176–180, 2007.
- [12] P. Thakur, H. Lu, S. Hsiao, and K. Johnson, "Automated optimal detection and classification of neural action potentials in extra-cellular recordings," *Journal of Neuroscience Methods*, vol. 162, no. 1-2, pp. 364–376, 2007.
- [13] D. Wagenaar and S. Potter, "Real-time multi-channel stimulus artifact suppression by local curve fitting," *Journal of neuroscience methods*, vol. 120, no. 2, pp. 113–120, 2002.
- [14] A. Grunmet, J. Wyatt, and J. Rizzo, "Multi-electrode stimulation and recording in the isolated retina," *Journal of neuroscience methods*, vol. 101, no. 1, pp. 31–42, 2000.
- [15] Y. Jimbo, H. Robinson, and A. Kawana, "Strengthening of synchronized activity by tetanic stimulation in cortical cultures: application of planar electrode arrays," *Biomedical Engineering, IEEE Transactions on*, vol. 45, no. 11, pp. 1297–1304, 1998.
- [16] Y. Jimbo and A. Kawana, "Electrical stimulation and recording from cultured neurons using a planar electrode array," *Bioelectrochemistry and Bioenergetics*, vol. 29, no. 2, pp. 193–204, 1992.
- [17] M. Ruaro, P. Bonifazi, and V. Torre, "Toward the neurocomputer: Image processing and pattern recognition with neuronal cultures," *Biomedical Engineering, IEEE Transactions on*, vol. 52, no. 3, pp. 371–383, 2005.
- [18] U. Egert and T. Meyer, *Heart on a Chip - Extracellular Multielectrode Recordings from Cardiac Myocytes in Vitro*. Springer Berlin Heidelberg, 2005, ch. Heart on a Chip - Extracellular Multielectrode Recordings from Cardiac Myocytes in Vitro, pp. 432–453.
- [19] A. Daus, M. Goldhammer, P. Layer, and C. Thielemann, "Electromagnetic exposure of scaffold-free three-dimensional cell culture systems." *Bioelectromagnetics*, vol. 32, no. 5, pp. 351–359, 2011.

- [20] R. Bestel, A. Daus, and C. Thielemann, "A novel automated spike sorting algorithm with adaptable feature extraction," *Journal of Neuroscience Methods*, vol. 211, no. 1, pp. 168–178, 2012.
- [21] G. Wang, Y. Zhou, A. Chen, P. Zhang, and P. Liang, "A robust method for spike sorting with automatic overlap decomposition," *Biomedical Engineering, IEEE Transactions on*, vol. 53, no. 6, pp. 1195–1198, 2006.
- [22] J. Choi, H. Jung, and T. Kim, "A new action potential detector using the mteo and its effects on spike sorting systems at low signal-to-noise ratios," *Biomedical Engineering, IEEE Transactions on*, vol. 53, no. 4, pp. 738–746, 2006.
- [23] R. Quiroga, Z. Nadasdy, and Y. Ben-Shaul, "Unsupervised spike detection and sorting with wavelets and superparamagnetic clustering," *Neural Computation*, vol. 16, pp. 1661–1687, 2004.
- [24] P. Horton, A. Nicol, K. Kendrick, and J. Feng, "Spike sorting based upon machine learning algorithms (soma)," *Journal of neuroscience methods*, vol. 160, no. 1, pp. 52–68, 2007.
- [25] R. Vogelstein, K. Murari, P. Thakur, C. Diehl, S. Chakrabarty, and G. Cauwenberghs, "Spike sorting with support vector machines," in *Engineering in Medicine and Biology Society, 2004. IEMBS'04. 26th Annual International Conference of the IEEE*, vol. 1. IEEE, 2004, pp. 546–549.
- [26] C. Legendy and M. Salcman, "Bursts and recurrences of bursts in the spike trains of spontaneously active striate cortex neurons," *Journal of neurophysiology*, vol. 53, no. 4, pp. 926–939, 1985.
- [27] L. Turnbull, E. Dian, and G. Gross, "The string method of burst identification in neuronal spike trains," *Journal of neuroscience methods*, vol. 145, no. 1-2, pp. 23–35, 2005.
- [28] Y. Chagnac-Amitai, H. Luhmann, and D. Prince, "Burst generating and regular spiking layer 5 pyramidal neurons of rat neocortex have different morphological features," *The Journal of Comparative Neurology*, vol. 296, no. 4, pp. 598–613, 1990.
- [29] S. Martinoia, P. Massobrio, M. Bove, and G. Massobrio, "Cultured neurons coupled to microelectrode arrays: circuit models, simulations and experimental data," *Biomedical Engineering, IEEE Transactions on*, vol. 51, no. 5, pp. 859–863, 2004.
- [30] M. Corner, J. Van Pelt, P. Wolters, R. Baker, and R. Nuytinck, "Physiological effects of sustained blockade of excitatory synaptic transmission on spontaneously active developing neuronal networks—an inquiry into the reciprocal linkage between intrinsic biorhythms and neuroplasticity in early ontogeny," *Neuroscience & Biobehavioral Reviews*, vol. 26, no. 2, pp. 127–185, 2002.
- [31] R. Baker, M. Corner, and J. van Pelt, "Spontaneous neuronal discharge patterns in developing organotypic mega-co-cultures of neonatal rat cerebral cortex," *Brain research*, vol. 1101, no. 1, pp. 29–35, 2006.
- [32] D. Wagenaar, T. DeMarse, and S. Potter, "Meabench: A toolset for multi-electrode data acquisition and on-line analysis," in *Neural Engineering, 2005. Conference Proceedings. 2nd International IEEE EMBS Conference on*. IEEE, 2005, pp. 518–521.
- [33] D. Tam, "An alternate burst analysis for detecting intra-burst firings based on inter-burst periods," *Neurocomputing*, vol. 44, pp. 1155–1159, 2002.

- [34] M. Jungblut, W. Knoll, C. Thielemann, and M. Pottek, "Triangular neuronal networks on microelectrode arrays: an approach to improve the properties of low-density networks for extracellular recording," *Biomedical Microdevices*, vol. 11, no. 6, pp. 1269–1278, 2009.
- [35] D. Eytan and S. Marom, "Dynamics and effective topology underlying synchronization in networks of cortical neurons," *The Journal of neuroscience*, vol. 26, no. 33, pp. 8465–8476, 2006.
- [36] J. Rolston, D. Wagenaar, and S. Potter, "Precisely timed spatiotemporal patterns of neural activity in dissociated cortical cultures," *Neuroscience*, vol. 148, no. 1, pp. 294–303, 2007.
- [37] J. van Pelt, P. Wolters, W. Rutten, M. Corner, P. Van Hulten, and G. Ramakers, "Spatio-temporal firing in growing networks cultured on multi-electrode arrays," in *World Congress on Neuroinformatics 2001*, 2001.
- [38] R. Segev, M. Benveniste, E. Hulata, N. Cohen, A. Palevski, E. Kapon, Y. Shapira, and E. Ben-Jacob, "Long term behavior of lithographically prepared in vitro neuronal networks," *Physical review letters*, vol. 88, no. 11, p. 118102, 2002.
- [39] J. Cohen, "Weighted kappa: Nominal scale agreement provision for scaled disagreement or partial credit," *Psychological bulletin*, vol. 70, no. 4, pp. 213–220, 1968.

Construction of The Sampled Signal Up To Any Frequency While Keeping The Sampling Rate Fixed

Dr. Ziad Sobih
Northeastern University
Boston, USA

sobih84@gmail.com

Prof. Martin Schetzen
MIT
Boston, USA

Abstract

In this paper we will try to develop a method that will let us construct up to any frequency by some additional work we propose. With this method we can construct up to any frequency by adding more hardware to the system with the same sampling rate. By increasing the hardware complexity and keeping the same sampling rate we can reduce the information loss in a proportional manner.

Keywords: Sampling, Filtering, Aliasing, Reconstruction, Heterodynes.

1. INTRODUCTION

Technically, we are proposing to decompose a signal into several separate signals by band passing the original signal. We then propose to process each signal and then to recombine the several processed signals. All this processing is being done in order to use a smaller sampling rate. There are several problems associated with this procedure that must be discussed in a paper on the procedure. First, practical band pass filters are only approximations of ideal band pass filters. We must discuss the effect of this approximation. Second, there is a lot of processing in the proposed method. We then must compare this method with others.

2. METHODOLOGY

In this method the input signal $x(t)$ is applied to many channels. The first channel with a pre-pass (low pass) filter with a frequency band from 0 to $F_s/2$ Hz. the second channel with a second pre-pass (band pass) filter with a frequency band from $F_s/2$ to F_s . The third channel with a pre-pass (band pass) and a frequency band from; F_s to $3F_s/2$, and so on up to n -channels; where the number of channels n is choose to satisfy the maximum frequency component of the output for the reconstructed signal. In this way we can divide the spectrum of the signal into intervals each with $F_s/2$ band starting from 0. Now if we sample the output of each filter at F_s then taking the DFT for each channel samples we will get a spectrum from 0 to $F_s/2$ for each channel output. At this point if the spectrum of odd channels i.e. the frequency band that lies in range $[mF_s < f < (m+1/2)F_s]$ is placed into the interval band of the pre pass filter for that channel. And the mirror image of the spectrum around the $(F_s/2)$ axis for even channels i.e. $(m-1/2)F_s < f < mF_s$ is placed into the interval band of the pre pass for that channel. We will get the spectrum for $x(t)$ constructed up to any frequency if the channels cover that frequency. As we can see by some additional work developed, we can increase frequency limit for reconstruction of signals without increasing the sampling frequency F_s .

In this approach to the solution I tried to follow the guidelines. I divided the problem into two parts. One part is to try to solve the problem in the frequency domain the second is to try to solve it in the time domain.

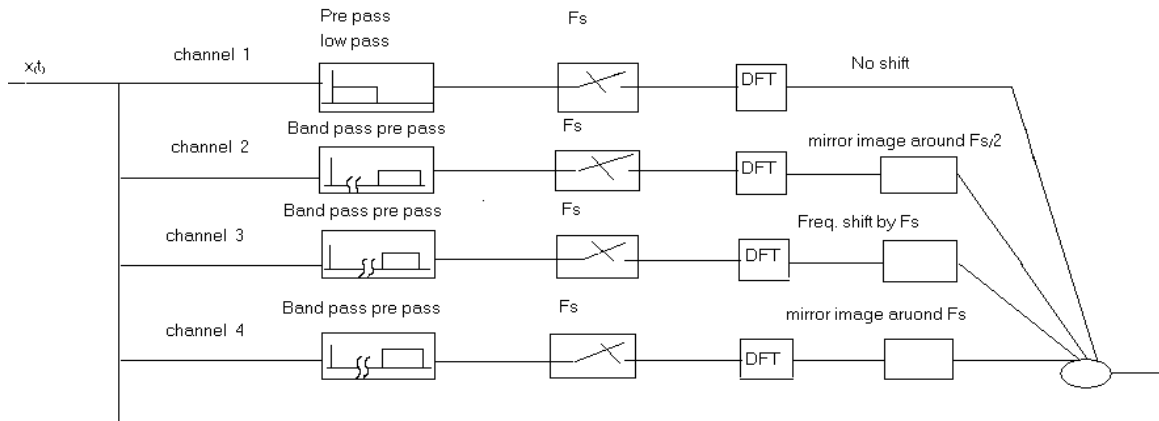


FIGURE 1: The System Block Diagram.

Because it is very hard, in practice, to build those ideal band pass filters. We suggest solving this problem by super heterodyning. By that I mean we build a high quality low pass filter with sharp transition with pass band from 0 to $F_s/2$ Hz. For the second channel we project the spectrum in the band $F_s/2$ to F_s into the band of the low pass filter. For the third channel we project the spectrum in the band F_s to $3F_s/2$ into the band of the low pass filter. And so on. I hope this will make us avoid the problem of having too many band pass filters which are difficult to have them ideal in practice.

let us suggest another method. Say we sample the original signal at a given rate, say F_s . Then shift the signal in time by a given amount and sample again at F_s . Again shift the signal in time and sample again at F_s . The samples from the various samplings of the original signal can then be combined by interlacing them to form a sample sequence equivalent to several times F_s . Note that the several samplings of the original signal can be done in parallel. My proposed technique would thus take no more time than sampling the original signal at the several times F_s . If this were done, my proposed technique is equivalent to replacing a sampler with a high sampling rate with several at a lower sampling rate. This procedure would thus avoid the problems involved with the other proposed procedure that I mentioned above.

I feel the time delay has to be logarithmic. The first channel is sampled every T_s . The second channel we delay by $T_s/2$ and sample again at F_s . For the third channel we have to delay now by $+T_s/4$ and $-T_s/4$ and sample each delayed wave at F_s . The two delays for the third channel is important to keep the sampling rate fixed and to be able to reconstruct the original signal by having equidistance samples, and so on.

Let me propose an alternative to this technique. Which does not require ideal band pass filters and reconstruction of the samplings of each band passed and frequency shifted waveform? I suggest just sampling the original waveform at a rate above F_n , the Nyquist rate, in the following manner: Call some time instant of the waveform $t = 0$. Then ;

1. Sample at the rate F_n with the first sample at $t = 0$.
2. Sample at the rate F_n with the first sample at $t = 1/(k)(F_n)$.
3. Sample at the rate F_n with the first sample at $t = 2/(k)(F_n)$.
4. Sample at the rate F_n with the first sample at $t = 3/(k)(F_n)$

and so forth until

$k-1$. Sample at the rate F_n with the first sample at $t = (k-1)/(k)(F_n)$.

Then concatenate the various sample sequences. Note that the resulting sequence obtained is the sequence that would be obtained by sampling the waveform at the rate $(k)(F_n)$. Note that this proposed technique does not require any filters, band shifting or time shifting of the waveform. Also, all the k samplings can be done at the same time if k samplers were used.

3. THEORY PROOF

To prove this proposed method we will take a cosine wave on the input of each interval band channel, as follows;

Channel 1

For an input; $X_1(t) = \cos(2\pi f_1 t)$

Where, $0 < f_1 < F_s/2$ and F_s is the sampling frequency

If the channel output is sampled at F_s rate then the output sampled signal will be

$X_1(n) = \cos(2\pi f_1 (n/F_s))$ and the reconstructed signal is the same as the input signal i.e.

$$X_1(t) = \cos(2\pi f_1 t)$$

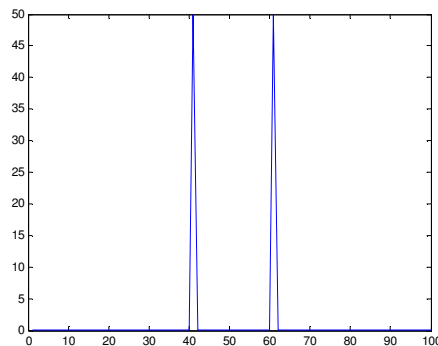


FIGURE 2: Digital Frequency $(f_1/F_s)=.4$.

Channel 2

For the input ; $X_2(t) = \cos(2\pi f_2 t)$

Where $F_s/2 < f_2 < F_s$ and F_s is the sampling frequency

The sampled signal will be

$$X_2(n) = \cos(2\pi (f_2/F_s) n)$$

$$X_2(n) = \cos(2\pi ((f_2/F_s)-1) n)$$

Reconstruction

$$X_2(t) = \cos(2\pi(f_2 - F_s)t)$$

Which is the mirror image of the input around $F_s/2$

We can get the input using the developed algorithm

$$X_2(t) = \cos(2\pi(F_s/2 + (F_s/2 - (f_2 - F_s))t))$$

$$X_2(t) = \cos(2\pi f_2 t)$$

Example : for $f_2 = 70$ Hz

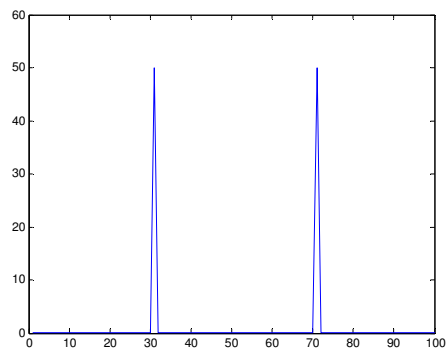


FIGURE 3: Digital frequency (f_2/F_s) = .7

Channel 3

For the input ; $X_3(t) = \cos(2\pi f_3 t)$

Where $F_s < f_3 < 3F_s/2$ and F_s is the sampling rate

The sampled signal is

$$X_3(n) = \cos(2\pi(f_3/F_s)n)$$

$$X_3(n) = \cos(2\pi((f_3/F_s) - 1)n)$$

The reconstructed signal is

$$X_3(t) = \cos(2\pi(f_3 - F_s)t)$$

Using our methodology and Shifting by F_s to place it in ch3 interval

$X_3(t) = \cos(2\pi f_3 t)$ which is the input

Example : For $F_3 = 130$ Hz

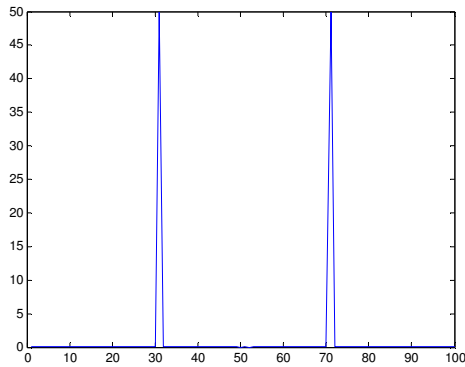


FIGURE 4: Digital Frequency (f_3/F_s) = 1.3.

Channel 4

For the input $X_4(t) = \cos(2\pi f_4 t)$

where $3F_s/2 < f_4 < 2F_s$ and the sampling rate is F_s

The digital signal after sampling is

$$X_4(n) = \cos(2\pi (f_4/F_s) n)$$

$$X_4(n) = \cos(2\pi (2 - (f_4/F_s)) n)$$

Reconstruction

$$X_4(t) = \cos(2\pi (2F_s - f_4) t)$$

Using our methodology For ch4 we have to take the mirror image around F_s

$X_4(t) = \cos(2\pi f_4 t)$ which is the same as the input

Example : for $f_4 = 190$ Hz

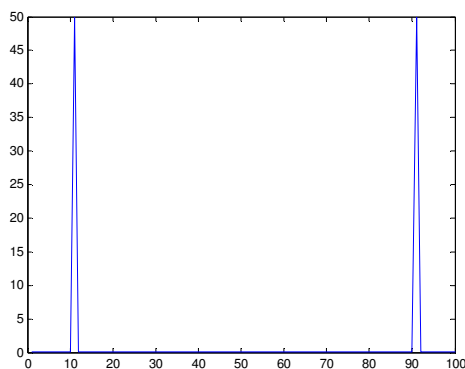


FIGURE 5: Digital Frequency (f_4/F_s) = 1.9.

$X(t) = X_1(t) + X_2(t) + X_3(t) + X_4(t)$, constructed up to $2F_s$ with F_s fixed

Using the same method we can construct up to any frequency as long as we cover the band with enough channels.

4. DISCUSSION

To have a feeling for this method think of a register where increasing the number of bits is like increasing the number of channels. Imagine that we are counting in the decimal system. This method is like inventing the zero. In this system each digit can take ten values. This is smaller to the sampling rate F_s . Increasing the hardware complexity by increasing the number of channels (i.e. increasing the number of bits (or digits) in a register) will enable us to construct up to higher frequency (more numbers or more accuracy)

5. IMPACT OF PROPOSED RESEARCH WORK

This work supports real time DSP. I will give a simple example. Let us say we have a sampler at 5kHz and we want to process a 20 kHz signal in real time. We can make four channels each one 5kHz band and proceed as explained above. This is like replacing the sampler by a 20 kHz sampler. The result of the simulation is given in figure 6 where we have two frequencies 4kHz and 16kHz sampled at 5kHz and reconstructed using our method at real time with no loss of information.

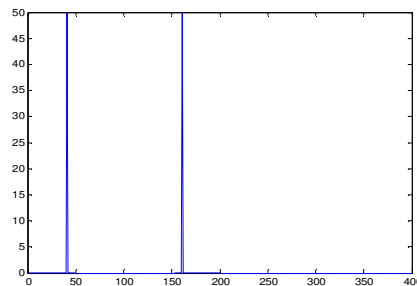


FIGURE 6: Test Using Two Frequencies.

6. COMPARATIVE EVALUATION

This idea was developed from Proakis Digital Communication book and the chapter on Multichannel and Multicarrier systems. There is a large amount of literature on multicarrier digital communication systems. Such systems have been implemented and used for over 35 years. One of the earliest systems, described by Doeltz et al. (1957) and called Kineplex, was used for digital transmission in the HF band. Other early work on multicarrier system design have been reported in the paper by Chang (1966). The use of DFT of multicarrier systems was proposed by Weinstein and Ebert (1971).

7. CONCLUSION

In this paper we were able to develop a procedure that will make us able to construct up to any frequency keeping the sampling frequency fixed. This is done by some additional steps we propose. We provide the proof for this method. A block diagram was given to the final system.

8. REFERENCES

- [1] A. Papoulis, Probability, Random Variables, and Stochastic Process, 2002.
- [2] J. G. Proakis, Digital Communications, 2001.
- [3] R. J. Schilling, Engineering Analysis, 1988.
- [4] H. L. Van Trees, Detection, Estimation, and Modulation Theory, 1968.

- [5] J. G. Proakis , Introduction to Digital Signal Processing ,1988.
- [6] C. Chen , Linear System Theory and Design , 1984.
- [7] S. Haykin , Communication System ,1983.
- [8] T. H. Glisson , Introduction to System Analysis , 1985.
- [9] Martin Schetzen, Airborne Doppler Radar, 2006.
- [10] Martin Schetzen, The Volterra & Wiener Theories of Nonlinear Systems, 2006.
- [11] Martin Schetzen, Discrete System using Matlab, 2004.

Rule Based Identification of Cardiac Arrhythmias from Enhanced ECG Signals Using Multi-Scale PCA

K. Sharmila

*Department of ECE
KITS Huzurabad
Karimnagar, India*

kothashama@yahoo.co.in

E. Hari Krishna

*Department of ECE
Kakatiya University
Warangal, India*

hari_etta@yahoo.co.in

K. Ashoka Reddy

*Department of E&I Engineering
KITS Warangal
Warangal, India*

reddy.ashok@yahoo.com

Abstract

The detection of abnormal cardiac rhythms, automatic discrimination from rhythmic heart activity, became a thrust area in clinical research. Arrhythmia detection is possible by analyzing the electrocardiogram (ECG) signal features. The presence of interference signals, like power line interference (PLI), Electromyogram (EMG) and baseline drift interferences, could cause serious problems during the recording of ECG signals. Many a time, they pose problem in modern control and signal processing applications by being narrow in-band interference near the frequencies carrying crucial information. This paper presents an approach for ECG signal enhancement by combining the attractive properties of principal component analysis (PCA) and wavelets, resulting in multi-scale PCA. In Multi-Scale Principal Component Analysis (MSPCA), the PCA's ability to decorrelate the variables by extracting a linear relationship and wavelet analysis are utilized. MSPCA method effectively processed the noisy ECG signal and enhanced signal features are used for clear identification of arrhythmias. In MSPCA, the principal components of the wavelet coefficients of the ECG data at each scale are computed first and are then combined at relevant scales. Statistical measures computed in terms of root mean square deviation (RMSD), root mean square error (RMSE), root mean square variation (RMSV) and improvement in signal to noise ratio (SNRI) revealed that the Daubechies based MSPCA outperformed the basic wavelet based processing for ECG signal enhancement. With enhanced signal features obtained after MSPCA processing, the detectable measures, QRS duration and R-R interval are evaluated. By using the rule base technique, projecting the detectable measures on a two dimensional area, various arrhythmias are detected depending upon the beat falling into particular place of the two dimensional area.

Keywords: ECG, Wavelet Transform, Principle Component Analysis, Arrhythmia Detection.

1. INTRODUCTION

In clinical applications, the arrhythmia condition, disturbing the rhythmic activity of heart, and its detection plays a vital role for diagnosing the patient's rhythmic status. The detection of abnormal cardiac rhythms became a potential area in clinical research. Arrhythmia detection is possible by analyzing the electrocardiogram (ECG) signal features. Several detection algorithms have been proposed earlier for arrhythmia detection, such as pattern matching, pattern subtraction etc., Rule base technique is one of the simple methods which can be utilized for arrhythmia detection after

obtaining the denoised ECG signal. Most of the physiological processes manifest themselves as signals reflecting their activity. Heart generated electrocardiogram (ECG), muscle generated electromyogram (EMG) and brain generated electroencephalogram (EEG) are some biomedical signals of interest [1]-[2]. The ECG signal, recorded with an electrocardiograph, is an electrical manifestation of the contraction and relaxation of the heart. ECG signal, whose frequency band of interest is 0.05 to 100Hz, is corrupted by different artifacts, which include 50/60 Hz power line interference (PLI), EMG interference and baseline wandering. PLI affects the complete ECG making it difficult for measurement of QRS complex and the QT interval. In order to remove 60 Hz PLI, an LMS adaptive filter can be employed by setting the 60Hz-component as a reference signal, so as to adjust the filter coefficient until the error is minimized from the input signal where the 60Hz-component is included [3]-[6]. The EMG, due to random contraction of muscles, is a high frequency component distributed in a wide frequency band which cannot be removed with a simplified filtering operation. The baseline wander, which is a low-frequency noise resulting from sudden movement of the body and respiration, has the same frequency band as of the ST segment of the ECG signal. Hence baseline wander is to be eliminated for the precise measurement of the ST segment. As a usual pre-processing phase, the real ECG is band pass filtered in order to remove the corrupted noise and to recover the signal waves (P, QRS and T). However, it has been established that the power spectral density (PSD) of the QRS complex (5-15 Hz) overlap with the muscle noise, while the PSD of P and T waves overlap with that of respiration, blood pressure at low frequency band usually (0.1 to 1 Hz). These different artifacts prevent considerably the accurate analysis of the ECG signal and eventual diagnosis of cardiac anomalies.

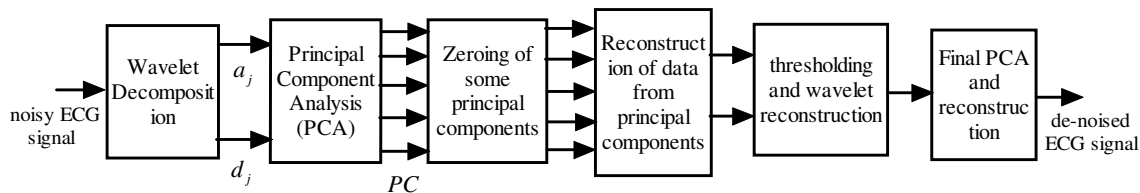


FIGURE 1: Block diagram for enhancement of ECG signal using multi-scale Principal Component Analysis.

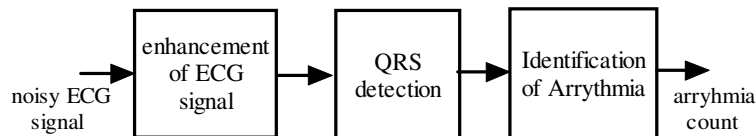


FIGURE 2: Block diagram for detection of cardiac arrhythmia from noisy ECG signal

Many solutions were reported in literature like digital filters (FIR or IIR), adaptive filtering methods and wavelet transform thresholding methods, in order to eliminate the noise of ECG signal [2]. The most widely used method, among the several other methods, used for ECG signal enhancement is the least mean square (LMS) adaptive algorithm [5]-[7]. But this algorithm is not able to track the rapidly varying non stationary signal, hence causes excessive low pass filter of mean parameters such as QRS complex. The wavelet transform (WT) has been proven to be a promising tool for non-stationary signal analysis, where in thresholding is used in wavelet domain to smooth out or to remove some coefficients of wavelet transform sub signals of the measured signal. Furthermore, the non-stationary behavior of the ECG signal, that becomes severe in the cardiac anomaly case, attracted researchers to analyze the ECG in both time and frequency planes simultaneously. The ability of the wavelet transform to explore signals into different frequency bands with adjustable time frequency resolution makes it suitable for ECG signal analysis and processing [8]-[13]. Many tools, methods and algorithms from signal processing theory have been proposed, described and implemented over the past few years to extract feature from ECG signals such as, total least squares based Prony modeling algorithm [14], correlation dimension and largest Lyapunov exponent [15], autoregressive model [16], multivariate autoregressive model [17], heartbeat interval combined with the shape and

morphological properties of the P, QRS and T waves [18], wavelet transform [19], multiple signal classification (MUSIC) algorithm [20], and efficient formation of morphological wavelet transform features together with the temporal features of the ECG signal [21].

Extracting the features from clean ECG signal has been found very helpful in identifying various cardiac arrhythmias. This could be difficult, when the size of the data of the ECG is huge and the existence of different noise types that may be contained in the ECG signals. Furthermore, manual analysis is considered a very time consuming and is prone to error. Hence arises the importance of automatic recognition and analysis of the ECG signals for extracting the different features available. Clean artifact free ECG signal is required exact identification of cardiac arrhythmias.

This paper presents multi-scale principal component analysis (MSPCA) based method for ECG enhancement as illustrated in Figure 1, which makes use of abilities of both the wavelets and the principal component analysis (PCA). This enhanced ECG is applied to the arrhythmia detector as shown in Figure 2. This basic idea is an extension to our previous work [22], where the enhanced ECG when presented to rule based arrhythmia classifier, resulted in a robust classification for arrhythmia.

2. WAVELETS

Since the useful ECG signal is corrupted with artifacts, the objective is to analyze accurately an ECG signal, to identify all the possible cardiovascular abnormalities. Wavelet analysis answers most of these problems [9]-[10]. In contrast to the classical Short-Time Fourier Transform (STFT) or Gabor transform, which uses a single analysis window, the WT uses long windows at low frequencies and short windows at high frequencies.

Discrete Wavelet Transform is referred as decomposition by wavelet filter banks as shown in Fig 3. and reconstruction in fig 4. Furthermore, the decomposition process, by which the signal is broken into many levels of lower resolution components, is iterative.

Only the last level of approximation is save among all levels of details, which provides sufficient data. A_j is the approximate coefficients and D_j is the detailed coefficients. The output coefficients of the LPF are referred to as 'approximations' and the output coefficients of the HPF are referred to as 'details'. The approximations of the signal are define its identity, while the details imparts gradation.

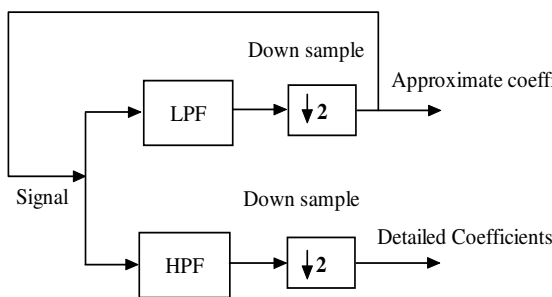


FIGURE 3: Wavelet Decomposition.

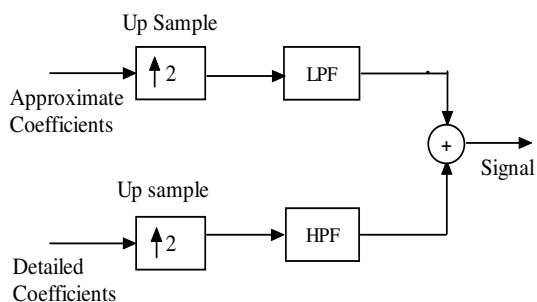


FIGURE 4: Wavelet Reconstruction.

Selecting a mother wavelet which closely matches the signal to be processed is of important in wavelet applications. The Haar wavelet algorithm is simple to compute, where the Daubechies algorithm is conceptually more complex and picks up detail that is missed by the Haar wavelet algorithm [11]. In practice, there is no absolute of choosing a certain wavelet. The choice of the wavelet function absolutely depends on the application. The energy spectrum of Daubechies

wavelet family is concentrated around low frequencies and more over similar in shape to QRS complex.

2.1 Wavelet De-noising

During denoising, the signals are transformed, thresholded and inverse-transformed as shown in Fig 5. The result is cleaned-up signal that shows important details. The general de-noising procedure follows the steps described below.

- i. *Decomposition*: Perform wavelet decomposition by choosing a mother wavelet and a convenient level N for decomposition.
- ii. *Thresholding detail coefficients*: For each level from 1 to N, select a threshold and apply soft or hard thresholding to the detail coefficients.
- iii. *Reconstruction*: Perform the wavelet reconstruction using the original approximation coefficients and the modified detail coefficients obtained at different levels.

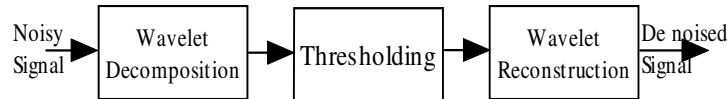


FIGURE 5: Wavelet Denoising Procedure.

There are two important issues with this: how to choose the threshold, and how to perform the thresholding [13]. Thresholding algorithm can be applied in two ways. One is hard thresholding process, which sets any wavelet coefficient less than or equal to the threshold to zero and the other is soft thresholding, which in addition to applying hard threshold, subtracts the threshold from any wavelet coefficient greater than the threshold.

2.2 Principal Component Analysis

Principal component analysis (PCA) is essentially a variable reduction procedure and it identifies the patterns in the data [27]. PCA can be performed using two methods, one of which using covariance matrix and the other using singular value decomposition (SVD). The essential steps involved in performing PCA on the data are discussed below.

Form a data set by using the periodicity of the ECG signal. Periodicity will be found using SVR profile i.e. the ratio of first principal component to the second principal component. The data matrix X is size of $m \times n$, where n is the SVR computed periodicity and m is the number of periods considered.

$$\text{Let } X(t) = [x_1(t), x_2(t), x_3(t), \dots, x_m(t)] \quad (1)$$

is the time ordered collection of the feature at all beats into a single matrix to which PCA can be applied. The means of the x_i are removed and the covariance matrix computed. The covariance is defined as

$$\Sigma = \frac{1}{n} [X X^T] \quad (2)$$

Σ is an $m \times m$ square symmetric matrix, eigenvalues (λ_j) and corresponding eigenvectors (\mathbf{a}_j) will be calculated, In general, once eigenvectors are found from the covariance matrix, the next step is to order them by eigenvalue, highest to lowest. This gives you the components in order of significance. The lesser eigenvalues can be ignored; this will form the basis for compression. The principal components (PC) are ordered eigenvectors of the covariance matrix. The PCs were obtained using

$$z_j = \mathbf{a}_j^T x \quad j=1, 2, \dots, n \quad (3)$$

The PCs are a linear transformation of the beats with transformation coefficients given by the eigenvectors α_j . The performance of PCA can further be improved by using PCA in conjunction with the wavelets, resulting in the concept of multiscale PCA.

2.3 Multi-Scale PCA

Multi-scale Principal Component Analysis (MSPCA) has been proposed as a fault detection method for the time series data [23]. This method combines the ability of PCA to extract the relationship among variables, then, to decorrelate the cross-correlation with that of wavelet analysis to decompose the time-series data into several frequency scales. Multiscale PCA reconstructs simplified multivariate signal, starting from a multivariate signal using a simple representation at each resolution level. In MSPCA, the PCA will be performed (i) on the matrices of details of different levels, (ii) on the matrices of coarser approximation coefficients and (iii) on the final reconstructed matrix. Finally, the interested simplified signals can be obtained by retaining useful principal components. Such an approach is developed in this paper by efficiently combining the abilities of PCA and wavelets. The present work is focused on using wavelets for multi scale data analysis. The sequence of steps employed for implementing proposed MSPCA method for ECG signal enhancement are given below.

Step 1: For each column in data matrix of ECG, perform wavelet decomposition process

Step 2: For each scale, compute covariance matrix of wavelet coefficients

Step 3: At selected scale, compute PCA loadings and scores of wavelet coefficients

Step 4: Select the appropriate number of loadings and wavelet coefficients (larger than appropriate threshold)

Step 5: For all scales together, compute PCA by including the scales with significant events

Step 6: Reconstruct approximate data matrix from the selected and thresholded scores at each scale

3. ARRHYTHMIA DETECTION

Arrhythmia is a condition in which the rhythmic activity of heart is disturbed. It may be due to disturbance in impulse formation or conduction or both but it is not always an irregular heart activity. Arrhythmia can be detected by analyzing the ECG signal features particularly based on the detectable measures, QRS duration and R-R interval. The detection of abnormal cardiac rhythm, an automatic discrimination from rhythmic heart activity became a thrust area in clinical research. Several detection algorithms have been proposed earlier for arrhythmia detection, such as pattern matching, pattern subtraction etc., Rule base technique is one of the simple method which can be utilized for arrhythmia detection after obtaining the denoised ECG signal. In the present work, initially, noisy ECG signal is effectively processed by the MSPCA method for noise elimination from corrupted signals. The detectable measures, QRS duration and R-R interval, are evaluated for the restored artifact free ECG signal. Based upon these two values, arrhythmia can be detected by using rule base technique (two- parameter method). The rule base technique essentially projects QRS duration and R-R intervals on a two dimensional area. According to the beat falling into particular place of this two dimensional area, various arrhythmias can be detected. The two- parameter mapping method [27] can be clearly described by using the Figure 6 shown below.

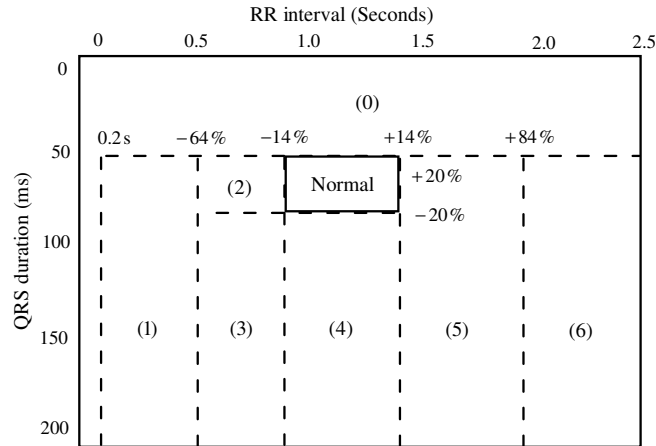


FIGURE 6: Two-Parameter Mapping.

In this two-parameter mapping, a region called normal is established by permitting the algorithm to first learn on a set of eight QRS complex defined by a clinician, as having normal rhythm and morphology for the specific subject. This learning establishes the initial center of the normal region in the two dimensional mapping space. Boundaries of all other regions in the map, except for region “0”, are computed as percentages of the location of the center of the normal region. Region “0” has fixed boundaries based on physiological limits. Any point mapped into region “0” is consider to be noise because it falls outside, what we normally expect to be the physiological limits of the smallest possible RR interval or QRS duration.

An abnormality such as tachycardia condition causes the clusters of beats to fall in the region “1” (which represents very short RR intervals) whereas the bradycardia beats fall in region“6”. Abnormalities must be classified by considering sequences of beats .for example a pre mature ventricular contraction (PVC) with a full compensatory pause would be characterized by a short RR interval coupled with a long QRS duration, followed by a long RR interval coupled with a normal QRS duration. This would be manifested as a sequence of two points on the map, the first in the region “3” and the second in the region “5”. Thus, arrhythmia analysis consists of analyzing the ways in which the beats fall onto the mapping space.

S.No	Type of Beat	Description
1.	Normal	If a beat falls in the normal box
2.	Asystole	No R wave for more than 1.72 s; less than 35 beats /min
3.	Dropped	A long RR interval;beat falls in region 6
4.	R-on-T	A beat falls in region 2
5.	Compensated PVC	A beat in Region 3, followed by another in Region 5
6.	Uncompensated PVC	A beat in Region 3, followed by another in the normal region
7.	Couplet	Two consecutive beats in region 3 followed by beat in normal region 5
8.	Paroxysmal bradycardia	If there are at least three consecutive points in Region 5
9.	Tachycardia	Average RR interval is less than 120 beats /min
10.	Fusion	Beat with a wide QRS duration; falls in region 4
11.	Escape	Beat with a delayed QRS complex; falls in Region 5
12.	Rejected	Beat with RR interval of 200 ms or less QRS duration of 60 ms or less.

TABLE 1: Arrhythmia Classification.

The center of the normal region is continuously updated, based on the average RR interval of the eight most-recent beats classified as normal. This approach permits the normal region to move in the two-dimensional space with normal changes in heart rate that occur with exercise and other physiological changes. The boundaries of other regions are modified beat-by-beat (adapts to normal changes in heart rate). The classification of the waveforms can be made by noting the regions in which successive beats fall. The rule base technique described above is an efficient method for extracting RR interval and QRS duration information from an denoised ECG signal. Based on the acquired information, different arrhythmias are classified as shown in the Table I.

4. RESULTS AND DISCUSSION

In order to test the performance of the proposed MSPCA algorithm, the MIT-BIH Arrhythmia Database records [24] were considered. To observe the enhancement, elimination of EMG, baseline wandering and PLI noise were considered. Steps described in section III were applied on corrupted ECG signals. Figure 7 illustrates EMG corrupted and eliminated ECG signal using multi scale PCA on two different subjects. Similarly, for the baseline wandering noise the result is shown in Fig 8. PLI corrupted and eliminated signals for two different subjects are portrayed in Fig 9. The principal components of the transformed ECG signal corresponding to record-103m are shown in Figure 10.

In order to test the efficacy of the proposed filtering method, different wavelets were used in the process of applying multi scale PCA on the PLI corrupted ECG and the resulted denoised signals were observed, wherein the morphological features of the ECG were clearly restored can be seen from fig 11. For the sake of comparison, the same ECGs were processed with only wavlets and the signals are portrayed as (e)-(g) in Figure 10. However, visual inspection of the enhanced signals did not reveal much information about the efficacy of the method used. Hence, for performance comparison, the following statistical measures were considered: RMSV, RMSE, RMSD.

1. Root mean square deviation (RMSD): It is the RMS value obtained from difference of pure ECG signal and the restored ECG signal that has been processed by the proposed method.

2. Root mean square error (RMSE): RMSE is the RMS value of the restored ECG minus filter output for clean ECG.

3. Root mean square variation (RMSV): It is the RMS value of the difference between the original input ECG and processed one.

A smaller values for RMSD, RMSE and RMSV indicates a better efficacy of the method in eliminating PLI and less distortion of signal after the processing; a lesser distortion of ECG morphology after the filtering operation; and less degree of variation of the ECG signal processed by the method respectively. In addition the restoring capacity can be evaluated using the effective measure, improvement in signal to noise ratio (SNRI).

4. Improvement in Signal to Noise Ratio (SNRI): It is the difference between Signal to Noise Ratio at Output (SNRout) in dB and the SNRinput in dB.

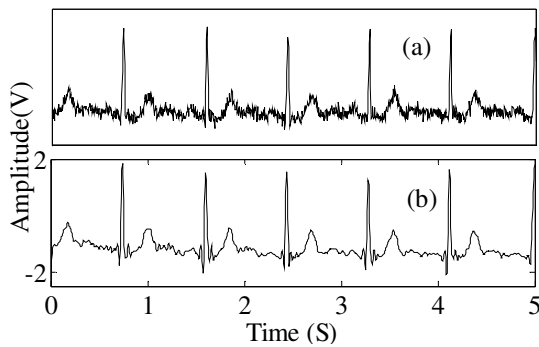


FIGURE 7: EMG corrupted ECG signal in trace (a) and eliminated ECG in trace (b) for two different subjects.

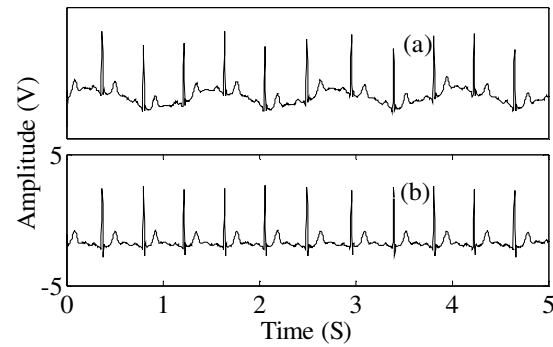


FIGURE 8: Baseline corrupted ECG signal in trace (a) and eliminated ECG in trace (b) for two different subjects.

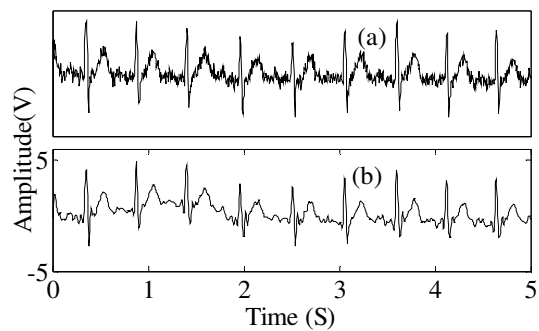
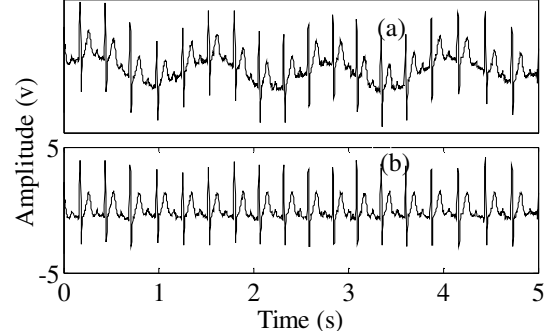


FIGURE 9: PLI corrupted ECG signal in trace (a) and eliminated ECG in trace (b) for two different subjects.



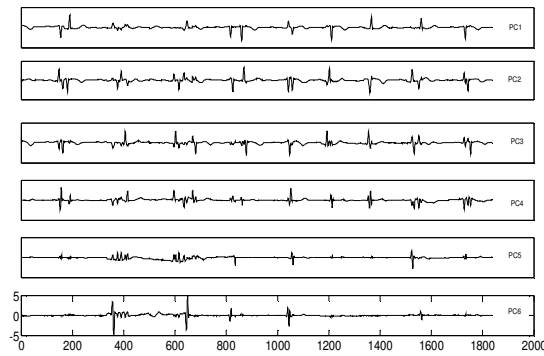


FIGURE 10: The Principle components of the transformd ECG record-103m.

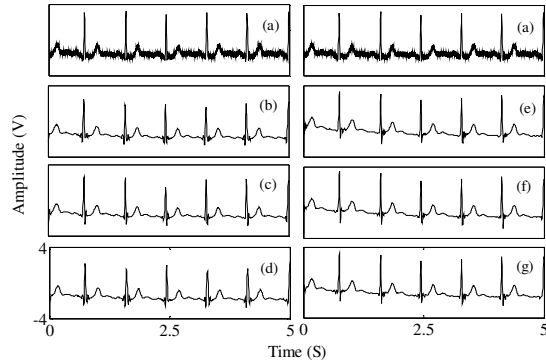


FIGURE 11: (a) PLI corrupted ECG and (b) PLI eliminated using Daubechies wavelet –MSPCA (c) Biorthogonal wavelt -MSPCA (d) coif wavelt- MSPCA (e) only Daubechies wavelet (f) only biorthogonal wavelet (g) only coif wavelet.

$$SNR_{Input} = 10 \log_{10} \left[\frac{\sum_i [x_n(i)]^2}{\sum_i [x_n(i) - x(i)]^2} \right] \quad (4)$$

$$SNR_{Output} = 10 \log_{10} \left[\frac{\sum_i [x_d(i)]^2}{\sum_i [x_d(i) - x(i)]^2} \right] \quad (5)$$

Where $x_n(i)$ is the noisy ECG signal, $x_d(i)$ is the de noised ECG signal and $x(i)$ is the Original ECG signal.

To evaluate these measures, all the wavelets were initially applied on the original uncorrupted MIT-BIH Arrhythmia and then on the PLI corrupted ECG. The computed RMS statistics for MSPCA were compared with pure wavelet transform based ECG enhancement algorithm.

Tables II - V, revealed that MSPCA resulted in better statistics compared to only wavelets, which eventually facilitates accurate ECG signal analysis due to improved restoration of ECG morphology. Also the Daubechies wavelet based PCA efficiently eliminated the PLI. After enhancement, based on the signal's QRS duration and a rule base, the identification of cardiac arrhythmias will performed. Two original ECG records (# record 103m, # record 215m), were enhanced by MSPCA, QRS locations and susequent classification is shown in Figure 12.

The sensitivity and positive predictivity of the beat detection algorithm are computed by

$$Se = \frac{TP}{TP + FN} \quad (6)$$

$$+P = \frac{TP}{TP + FP} \quad (7)$$

where TP is the number of true positives, FN the number of false negatives, and FP the number of false positives. The sensitivity Se reports the percentage of true beats that were correctly

detected by the algorithm. The positive predictivity +P reports the percentage of beat detections which were in reality true beats.

Table VI and Table VII give sensitivity and positive predictivity data for different cardiac arrhythmias.

ECG Data base	WAVELET			MSPCA		
	db5 (Soft)	coif5 (Soft)	bior6.8 (Hard)	db5 (Soft)	coif5 (Soft)	bior6.8 (Hard)
103	0.005± 1.5x10-4	0.005 ± 2.4 x10-4	0.002 ± 5.0 x10-4	0.004± 1.3x10-4	0.004 ± 2.2 x10-4	0.001± 2.9x10-4
215	0.005 ± 1.5 x10-4	0.003± 2.4 x10-4	0.004 ± 3.0 x10-4	0.004 ± 1.3 x10-4	0.003 ± 2.3 x10-4	0.003 ± 2.8 x10-4
219	0.005 ± 1.5 x10-4	0.004 ± 2.4 x10-4	0.004 ± 3.0 x10-4	0.004 ± 1.4x10-4	0.003 ± 2.3 x10-4	0.003± 2.8x10-4
222	0.005 ± 1.5 x10-4	0.005 ± 2.4 x10-4	0.149 ± 0.011	0.004 ± 1.4 x10-4	0.004 ± 2.3 x10-4	0.148 ± 0.010

TABLE 2: RMSV Measures.

ECG Data base	WAVELET			MSPCA		
	db5 (Soft)	coif5 (Soft)	bior6.8 (Hard)	db5 (Soft)	coif5 (Soft)	bior6.8 (Hard)
103	0.005 ± 1.5 x10-4	0.005 ± 2.4 x10-4	0.149 ± 0.011	0.004 ± 1.4 x10-4	0.004 ± 2.3 x10-4	0.148 ± 0.009
215	0.005 ± 1.5 x10-4	0.005 ± 2.4 x10-4	0.148 ± 0.011	0.004 ± 1.4 x10-4	0.004 ± 2.1 x10-4	0.147 ± 0.010
219	0.005 ± 1.5 x10-4	0.005 ± 2.4 x10-4	0.146 ± 0.011	0.003 ± 1.0 x10-4	0.003 ± 2.3 x10-4	0.145 ± 0.010
222	0.005 ± 1.5 x10-4	0.005 ± 2.4 x10-4	0.147± 0.011	0.004 ± 1.0 x10-4	0.004 ± 2.3 x10-4	0.146 ± 0.009

TABLE3: RMSE Measures.

ECG Data base	WAVELET			MSPCA		
	db5 (Soft)	coif5 (Soft)	bior6.8 (Hard)	db5 (Soft)	coif5 (Soft)	bior6.8 (Hard)
103	0.132 ± 0.008	0.132 ± 0.008	0.149 ± 0.011	0.132 ± 0.008	0.132 ± 0.008	0.148 ± 0.009
215	0.133 ± 0.007	0.005 ± 2.4 x10-4	0.148 ± 0.011	0.004 ± 1.4 x10-4	0.004 ± 2.1 x10-4	0.147 ± 0.010
219	0.131 ± 0.122	0.005 ± 2.4 x10-4	0.146 ± 0.011	0.003 ± 1.0 x10-4	0.131 ± 0.122	0.145 ± 0.010
222	0.005 ± 1.5 x10-4	0.005 ± 2.4 x10-4	0.147± 0.011	0.004 ± 1.0 x10-4	0.004 ± 2.3 x10-4	0.146 ± 0.009

TABLE 4: RMSD Measures.

ECG Data base	WAVELET			MSPCA		
	db5 (Soft)	coif5 (Soft)	bior6.8 (Hard)	db5 (Soft)	coif5 (Soft)	bior6.8 (Hard)
103	5.53	5.44	4.99	5.52	5.44	4.98
215	5.51	5.44	4.99	5.50	5.44	4.97
219	5.50	5.44	4.99	5.49	5.44	4.98
222	5.52	5.44	4.99	5.50	5.44	4.97

TABLE 5: SNRI Measures.

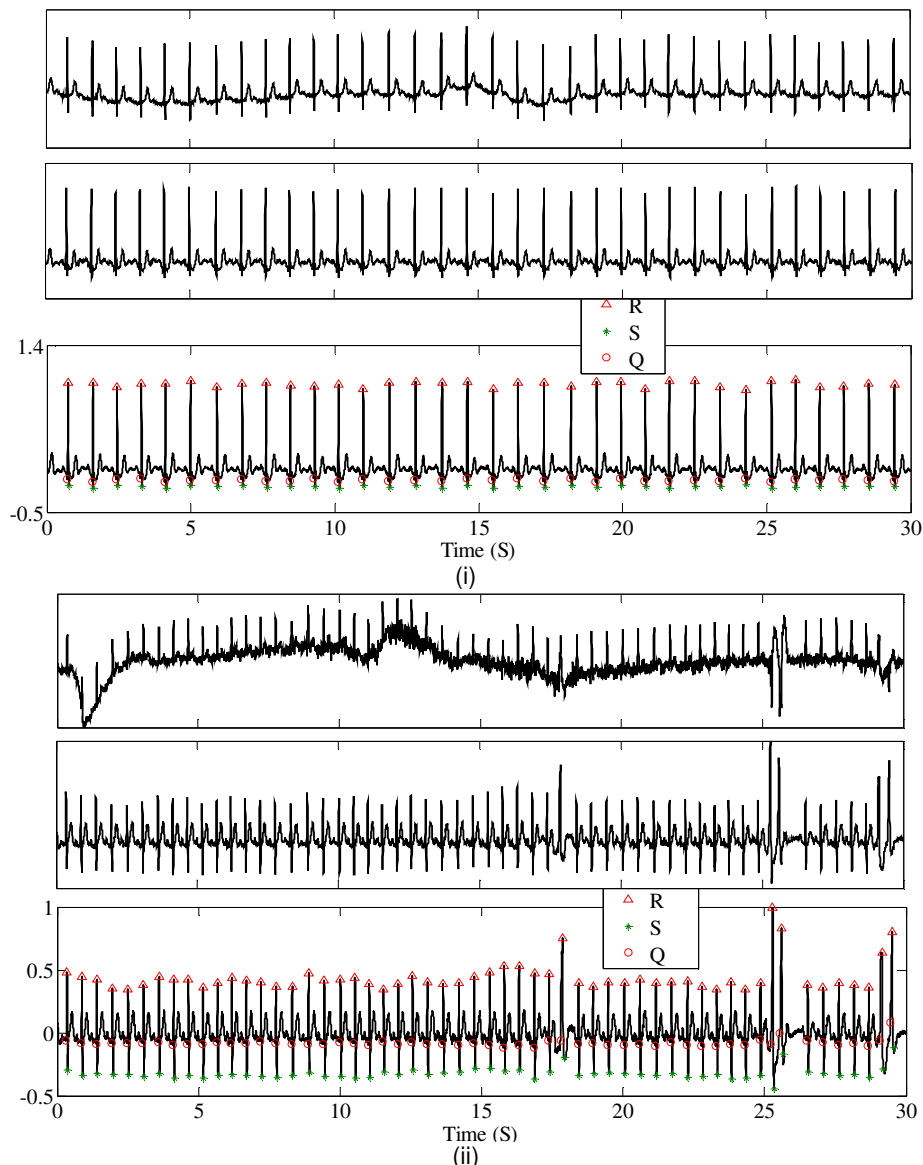


FIGURE 12: Noisy ECG signal shown in top trace, denoised using MSPCA in bottom trace and QRS detected signal in bottom trace for identification of cardiac arrhythmias for a record of 103m in (i) and a record of 215m.

record #	Bradycardia					Escape					Normal				
	TP	FP	FN	Se (%)	+P (%)	TP	FP	FN	Se (%)	+P (%)	TP	FP	FN	Se (%)	+P (%)
100m	32	1	0	96.96	100.00	65	0	1	100.00	98.48	562	2	0	99.64	100.00
101m	20	0	1	100.00	95.23	30	1	0	96.77	100.00	04	0	0	100.00	100.00
103m	170	0	1	100.00	99.41	232	1	2	99.57	99.14	1812	20	16	98.90	99.12
107m	1092	10	12	99.09	98.91	1435	12	14	99.17	99.03	58	1	0	98.30	100.00
121m	110	1	1	99.09	99.09	150	0	1	100.00	99.33	09	0	0	100.00	100.00
215m	154	0	1	100.00	99.35	295	1	0	99.66	100.00	2278	30	12	98.70	99.47
219m	494	1	0	99.79	100.00	1056	14	17	98.69	98.41	964	1	2	99.89	99.79
222m	613	2	1	99.67	99.83	1254	12	16	99.05	98.74	311	1	1	99.67	99.67
Total	2685	15	17	99.44	99.37	4517	40	41	99.12	99.10	5998	55	31	99.09	99.48

TABLE 6: Arrhythmia Beats of Eight Different Subjects.

record #	Noise					Fusion				
	TP	FP	FN	Se (%)	+P (%)	TP	FP	FN	Se (%)	+P (%)
100m	646	2	1	99.69	99.84	1069	20	2	98.16	99.81
101m	175	1	0	99.43	100	41	0	1	100.0	97.61
103m	162	1	1	99.38	99.38	43	0	1	100.0	97.72
107m	1486	25	24	99.00	99.06	175	1	1	99.43	99.43
121m	1017	10	2	99.02	99.80	257	1	2	99.61	99.22
215m	463	1	0	99.78	100.0	335	1	1	99.70	99.70
219m	140	0	1	100	99.29	39	0	0	100.0	100.0
222m	661	2	1	99.69	99.84	583	2	1	99.65	99.82
Total	4570	42	30	99.08	99.34	2542	25	9	99.02	99.64

TABLE 7: Arrhythmia Beats of Eight Different Subjects.

5. CONCLUSION

In clinical applications, the arrhythmia condition, disturbing the rhythmic activity of heart, and its detection plays a vital role for diagnosing the patient's rhythmic status. The detection of abnormal cardiac rhythms, automatic discrimination from rhythmic heart activity, became a thrust area in clinical research. Arrhythmia detection is possible by analyzing the electrocardiogram (ECG) signal features. ECG is a non-stationary biomedical signal that is invariably corrupted with different artifacts during its recording. This paper presents an approach for ECG signal

enhancement by combining the attractive properties of principal component analysis (PCA) and wavelet processing, called multiscale PCA. The resulting multi-scale PCA extracts relationships between the variables by PCA, and between the measurements by wavelet analysis. In this application, the proposed MSPCA served as a powerful tool when addressing problems related to noise elimination. MSPCA eliminated the different types of noises present in the corrupted ECG signal. Experimental results revealed that Daubechies based MSPCA resulted in improved restoration of ECG morphology compared to simple wavelet processing. With enhanced ECG signal features obtained after MSPCA processing, detectable measures, QRS duration and R-R interval are evaluated. By using the rule base technique, projecting the detectable measures on a two dimensional area, various arrhythmias were detected depending upon the beat falling into particular place of the two dimensional area.

6. REFERENCES

- [1] J. C. Huhta and J. G. Webster, "60-Hz interference in electrocardiograph," IEEE Trans. Biomed. Eng., vol. 20, pp. 91-101, 1973.
- [2] L. Sornmo and P. Laguna, Bioelectrical Signal Processing in Cardiac and Neurological Applications, Elsevier Academic Press, MA, USA, 2005.
- [3] S. C. Pie and C. C. Tseng, "Elimination of AC interference in electrocardiogram using IIR notch filter with transient suppression," IEEE Trans. Biomed. Eng., vol. 42, pp. 1128-2232, 1995.
- [4] Ch. Levkov, G. Mihov, R. Ivanov and I. Daskalov, "Subtraction of 50 Hz interference from the electrocardiogram,"
- [5] Med. & Biol. Eng. & Comp., vol. 22, pp. 371-373, 1984.
- [6] B. Widrow, "Adaptive noise cancelling: principles and applications," Proc. IEEE, vol. 63, (12), pp. 1692-1716, 1975.
- [7] A. K. Ziaranj and A. Konrad, "A nonlinear adaptive method of elimination of PLI in ECG signals," IEEE Trans. Biomed. Eng., vol. 49, (6), pp. 540-547, 2002.
- [8] P. S. Hamilton, "A comparison of adaptive and non-adaptive filters for the reduction of PLI in the ECG," IEEE Trans. Biomed. Eng., vol. 43(1), pp. 105-109, 1996.
- [9] L. Park, K. J. Lee and H. R. Yoon, "Application of a wavelet adaptive filter to minimize distortion of the ST-segment," Med. Biol. Eng. & Comput., vol. 36, no. 5, pp. 581- 586, September 1998.
- [10] Cuiwei Li, Chongxun Zheng, and Changfeng Tai, " Detection of ECG Characteristic Points using Wavelet Transforms," IEEE Trans. Biomed. Eng., Vol. 42, No. 1, 1995.
- [11] J.S Sahambi, S.N. Tandon and R.K.P. Bhatt, "Using Wavelet Transform for ECG Characterization," IEEE Eng. in Med. and Bio., 1997.
- [12] S.Z. Mohmoodabadi, A. Ahmadian, M.D. Abolhasani (2005) ECG feature extraction using daubechies wavelets, Proc. of the fifth IASTED International Conference, Benidorm, Spain.
- [13] M. Alfaouri and K. Daqrouq, "ECG signal denoising by wavelet transform thresholding," American Journal of Applied Sciences, vol. 5, no. 3, pp. 276-281, 2008.
- [14] D. L. Donoho, De-noising by softthresholding, IEEE Transaction on Information Theory, Vol. 41, pp. 613-627, May 1995.

- [15] SW Chen. "Two-stage discrimination of cardiac arrhythmias using a total least squares-based prony modeling algorithm" IEEE Transaction on Biomedical Engineering, 47: pp. 1317-1326, 2000.
- [16] Owis, M., Abou-Zied, A., Youssef, A.B., Kadah, Y., "Robust feature extraction from ECG signals based on nonlinear dynamical modeling," 23rd Annual International Conference IEEE Engineering in Medicine and Biology Society. (EMBC'01). Volume 2. pp. 1585–1588, 2001.
- [17] Dingfei Ge, Narayanan Srinivasan, Shankar Krishnan. "Cardiac arrhythmia classification using autoregressive modeling" BioMedical Engineering OnLine, 1(1):5, pp. 1585–1588, 2002.
- [18] GE Ding-Fei, HOU Bei-Ping, and XIANG Xin-Jian, "Study of Feature Extraction Based on Autoregressive Modeling in ECG Automatic Diagnosis", ACTA Automation Sinica. Vol. 33 No. 5. pp. 462-466, 2007.
- [19] P. de Chazal, M. O'Dwyer, and R. B. Reilly, "Automatic Classification of Heartbeats Using ECG Morphology and Heartbeat Interval Features," IEEE Transaction on Biomedical Engineering, Vol. 51, No. 7, pp.1196- 1206, July 2004.
- [20] Inan, O.T., Giovangrandi, L. and Kovacs, G.T.A., "Robust neuralnetwork-based classification of premature ventricular contractions using wavelet transform and timing interval features", IEEE Transaction on Biomedical Engineering, Vol. 53, No.12. pp. 2507-2515, 2006.
- [21] Ahmad R. Naghsh-Nilchi and A. Rahim Kadkhoda mohammadi, "Cardiac Arrhythmias Classification Method Based on MUSIC, Morphological Descriptors, and Neural Network", EURASIP Journal on Advances in Signal Processing, Article No. 202. Volume 2008.
- [22] K. Sharmila, E. H. Krishna, K. N. Reddy and K. A. Reddy, " Application of Multi-scale principal component analysis (MSPCA) for enhancement of ECG signals", in Proc. of 28th IEEE International Instrumentation and Measurement Technology Conf., I2MTC-2011, pp. 1540-1544, Hangzhou, China, 10-12 May, 2011.
- [23] Turker Ince, S. Kiranyaz, and M. Gabbouj, "A Generic and Robust System for Automated Patient-specific Classification of Electrocardiogram Signals", IEEE Transactions on Biomedical Engineering, Vol. 56, No. 5, May 2009.
- [24] F. Castells, P. Laguna, L. Sörnmo, A. Bollmann and J. Millet Roig. "Principal component analysis in ECG signal processing," EURASIP J. Adv. Si. Pr., vol. 2007.
- [25] B. R. Bakshi, "Multiscale PCA with application to multivariate statistical process monitoring, AIChE Journal, 44, 7, pp.1596-1610, 1998.
- [26] "The MIT-BIH Arrhythmia Database,"
<http://physionet.ph.biu.ac.il/physiobank/database/mitdb/>
- [27] V. X. Afonso, W. J. Tompkins, T. Q. Nguyen, and S. Luo, "ECG Beat detection using filter banks", IEEE Trans. on Biomed. Eng. , vol. 46, no.2. pp. 192-202,1999.

INSTRUCTIONS TO CONTRIBUTORS

The *International Journal of Signal Processing (SPIJ)* lays emphasis on all aspects of the theory and practice of signal processing (analogue and digital) in new and emerging technologies. It features original research work, review articles, and accounts of practical developments. It is intended for a rapid dissemination of knowledge and experience to engineers and scientists working in the research, development, practical application or design and analysis of signal processing, algorithms and architecture performance analysis (including measurement, modeling, and simulation) of signal processing systems.

As SPIJ is directed as much at the practicing engineer as at the academic researcher, we encourage practicing electronic, electrical, mechanical, systems, sensor, instrumentation, chemical engineers, researchers in advanced control systems and signal processing, applied mathematicians, computer scientists among others, to express their views and ideas on the current trends, challenges, implementation problems and state of the art technologies.

To build its International reputation, we are disseminating the publication information through Google Books, Google Scholar, Directory of Open Access Journals (DOAJ), Open J Gate, ScientificCommons, Docstoc and many more. Our International Editors are working on establishing ISI listing and a good impact factor for SPIJ.

The initial efforts helped to shape the editorial policy and to sharpen the focus of the journal. Started with volume 7, 2013, SPIJ appears with more focused issues related to signal processing studies. Besides normal publications, SPIJ intend to organized special issues on more focused topics. Each special issue will have a designated editor (editors) – either member of the editorial board or another recognized specialist in the respective field.

We are open to contributions, proposals for any topic as well as for editors and reviewers. We understand that it is through the effort of volunteers that CSC Journals continues to grow and flourish.

SPIJ LIST OF TOPICS

The realm of Signal Processing: An International Journal (SPIJ) extends, but not limited, to the following:

- Biomedical Signal Processing
- Communication Signal Processing
- Detection and Estimation
- Earth Resources Signal Processing
- Acoustic and Vibration Signal Processing
- Data Processing
- Digital Signal Processing
- Geophysical and Astrophysical Signal Processing
- Industrial Applications
- Multi-dimensional Signal Processing
- Optical Signal Processing
- Pattern Recognition
- Radar Signal Processing
- Remote Sensing
- Signal Filtering
- Signal Processing Systems
- Signal Processing Technology
- Signal Theory
- Software Developments
- Sonar Signal Processing
- Spectral Analysis
- Speech Processing
- Stochastic Processes

CALL FOR PAPERS

Volume: 7 - Issue: 5

i. Paper Submission: November 30, 2013 **ii. Author Notification:** December 25, 2013

iii. Issue Publication: December 2013

CONTACT INFORMATION

Computer Science Journals Sdn Bhd

B-5-8 Plaza Mont Kiara, Mont Kiara
50480, Kuala Lumpur, MALAYSIA

Phone: 006 03 6207 1607
006 03 2782 6991

Fax: 006 03 6207 1697

Email: cscpress@cscjournals.org

CSC PUBLISHERS © 2013
COMPUTER SCIENCE JOURNALS SDN BHD
B-5-8 PLAZA MONT KIARA
MONT KIARA
50480, KUALA LUMPUR
MALAYSIA

PHONE: 006 03 6207 1607
006 03 2782 6991

FAX: 006 03 6207 1697
EMAIL: cscpress@cscjournals.org